

CANADIAN JOURNAL OF RESEARCH

VOLUME 18

DECEMBER, 1940

NUMBER 12

CONTENTS

SECTION A.—PHYSICAL SCIENCES

	Page
Band Spectrum of the BN Molecule— <i>A. E. Douglas and G. Herzberg</i> - - - - -	179
Collimated Light Beams in Spectrophotometry— <i>G. O. Langstroth, W. W. Brown, and K. B. Newbould</i> - - - - -	186
INDEX, SECTION A, VOLUME 18.	

SECTION B.—CHEMICAL SCIENCES

Études Physico-chimiques sur les Carbonates Alcalins. II. Calcul des Coefficients d'Activité des Carbonates de Sodium et de Potassium, en Solution Aqueuse— <i>L. Lortie et P. Demers</i> - - - - -	373
The Phosphorus and Iodine Contents of British Columbia Fish Oils— <i>R. D. Heddle and J. S. Brawn</i> - - - - -	386
The Separation and Identification of the Compounds Present in a Turner Valley Crude Oil— <i>L. M. Watson and J. W. T. Spinks</i> - - - - -	388
A Proposed Modification of Emmerie's Iron-Dipyridyl Method for Determining the Tocopherol Content of Oils— <i>W. E. Parker and W. D. McFarlane</i> - - - - -	405
Studies on Homogeneous First Order Gas Reactions. XII. The Decomposition of Glyoxal Tetra-acetate— <i>J. C. Arnell, J. R. Dacey, and C. C. Coffin</i> - - - - -	410
The Alkaloids of Fumariaceous Plants. XXX. Aurotensine— <i>R. H. F. Manske</i> - - - - -	414
INDEX, SECTION B, VOLUME 18.	

NATIONAL RESEARCH COUNCIL
OTTAWA, CANADA

Publications and Subscriptions

The Canadian Journal of Research is issued monthly in four sections, as follows:

- A. Physical Sciences
- B. Chemical Sciences
- C. Botanical Sciences
- D. Zoological Sciences

For the present, Sections A and B are issued under a single cover, as also are Sections C and D, with separate pagination of the four sections, to permit separate binding, if desired.

Subscription rates, postage paid to any part of the world (effective 1 April, 1939), are as follows:

	<i>Annual</i>	<i>Single Copy</i>
A and B	\$ 2.50	\$ 0.50
C and D	2.50	0.50
Four sections, complete	4.00	—

The Canadian Journal of Research is published by the National Research Council of Canada under authority of the Chairman of the Committee of the Privy Council on Scientific and Industrial Research. All correspondence should be addressed:

National Research Council, Ottawa, Canada.

Notice to Contributors

Fifty reprints of each paper are supplied free. Additional reprints, if required, will be supplied according to a prescribed schedule of charges.





Canadian Journal of Research

Issued by THE NATIONAL RESEARCH COUNCIL OF CANADA

VOL. 18, SEC. A.

DECEMBER, 1940

NUMBER 12

BAND SPECTRUM OF THE BN MOLECULE¹

BY A. E. DOUGLAS² AND G. HERZBERG³

Abstract

In a discharge through helium with traces of boron trichloride and nitrogen two new band systems (a triplet system and a singlet system) were found which are shown to be due to the BN molecule. The first system represents a ${}^3\Pi - {}^3\Pi$ transition similar to the Swan bands of the C_2 molecule with which BN is iso-electronic. A vibrational and rotational analysis of this system is carried out and yields the formula for the heads:

$$\nu_H = 27775.8 + (1302.6 \nu' - 14.9 \nu'^2) - (1502.3 \nu'' - 12.3 \nu''^2)$$

and the B and α values and internuclear distances: $B_2' = 1.555$, $B_2'' = 1.666$, $\alpha' = 0.010$, $\alpha'' = 0.025$, $r_2' = 1.326$, $r_2'' = 1.281$. An analysis of the singlet system has not as yet been possible.

Introduction

While BN is a stable and well known chemical compound of very high melting point (2730°C.) and has a crystal structure very similar to that of graphite, no spectrum of the diatomic BN molecule has yet been recorded. To be sure, the bands observed in the flame that is produced by the action of active nitrogen on boron trichloride were at one time considered to be due to BN until it was shown by Mulliken (6), by means of the isotope effect, that they are due to BO. Recently in an investigation of the spectrum of the B_2 molecule we found incidentally that, when nitrogen was present as an impurity or was added artificially to a discharge through a mixture of helium and boron trichloride, a number of new bands occur which we can show are due to the BN molecule. The analysis of the bands has given information about the electronic structure as well as the vibrational frequencies and internuclear distances of this molecule.

Experimental

The discharge tube was the same as used in the work on the B_2 spectrum (3, 4). As there the tube was filled with helium of about 10 mm. pressure and a small amount of boron trichloride was admitted. If the helium contained a trace of nitrogen the spectra taken in the same way as for B_2 , that

¹ Manuscript received October 7, 1940.

Contribution from the Department of Physics, University of Saskatchewan, Saskatoon, Sask., with financial assistance from the National Research Council of Canada.

² Graduate student, holder of a Bursary (1939-1940) under the National Research Council of Canada.

³ Research Professor of Physics.

is, just before the typical helium colour was completely restored, showed a number of new bands in the region 3200 to 3900 Å in place of the B₂ bands.

The exposures were taken with the 20-ft. diffraction grating spectrograph of this department and measured with a Gaertner comparator.

Vibrational Structure of the Triplet System

A number of the red shaded bands found between 3430 and 3860 Å (see the spectrogram Fig. 1) showed clear triplet branches at some distance from the heads, and also the band heads seemed to be triple. In fact they were very similar in appearance to the bands of the second positive group of nitrogen which appeared on the same plates and which represent a ³Π-³Π transition (but they are shaded in the opposite direction). Each strong band head of the new system except the one at the centre (0-0 band) is accompanied by a weaker band, which is obviously due to the less abundant isotopic molecule B¹⁰N. The stronger bands are easily arranged in a Deslandres table as given in Table I. The positions of the weaker bands given in parentheses in Table I fit within the accuracy of measurement the positions expected on the assumption that they are due to B¹⁰N, whereas the main bands are due to B¹¹N. The figures in square brackets in Table I give the deviations observed—calculated for the isotopic bands. The calculated values have been obtained by assuming the formula given below for the main bands and using the well known formulae for the isotope shifts [see e.g., Herzberg (5)]. Account was taken of the variation of the distance between head and origin in these calculations (see the rotational analysis below).

In view of the fact that only band heads, which are not very sharp, could be measured, the accuracy of the observed isotope shifts is not sufficient to decide between the emitters BC, BN and BO. However, the fact that the bands are definitely triplet bands excludes BC and BO unambiguously. It

TABLE I
DESLANDRES TABLE OF THE BN BANDS
(Band heads of B¹¹N and B¹⁰N, the latter in parentheses)

$\begin{smallmatrix} v'' \\ v' \end{smallmatrix}$	0	1	2	3
0	27775.8 —	26286.0 (26244.0) [-.3]		
1	29063.8 (29096.8) [+.2]	27573.5 —	26106.9 (26060.3) [-.2]	
2		28831.4 (28856.7) [+.1]	27365.2 —	25925.7 —
3			28593.8 (28611.7) [+.5]	27152.9 —

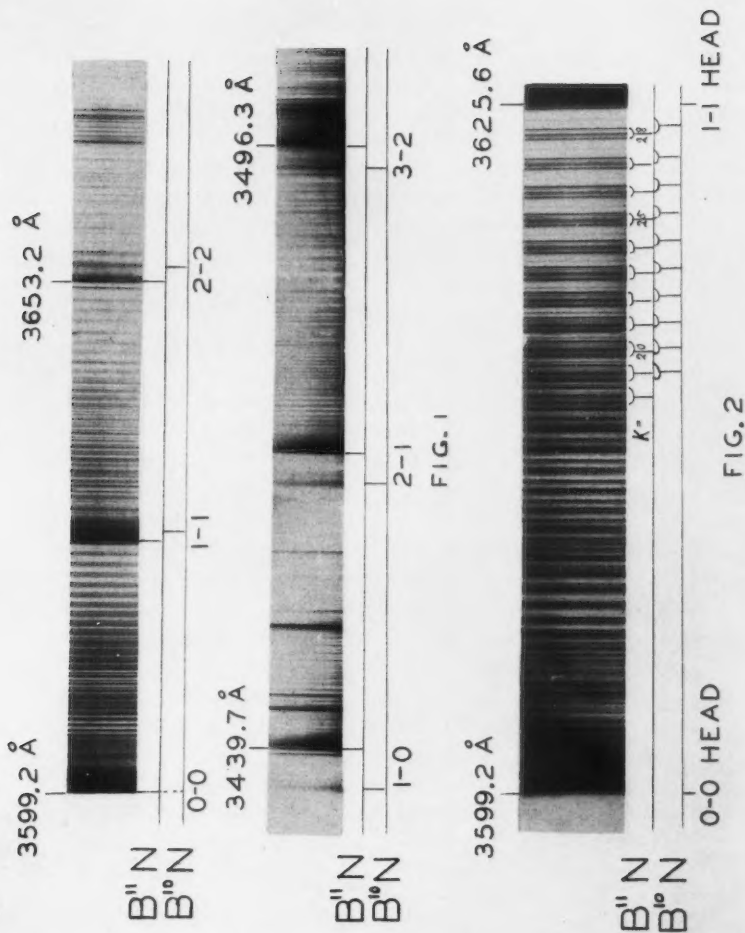
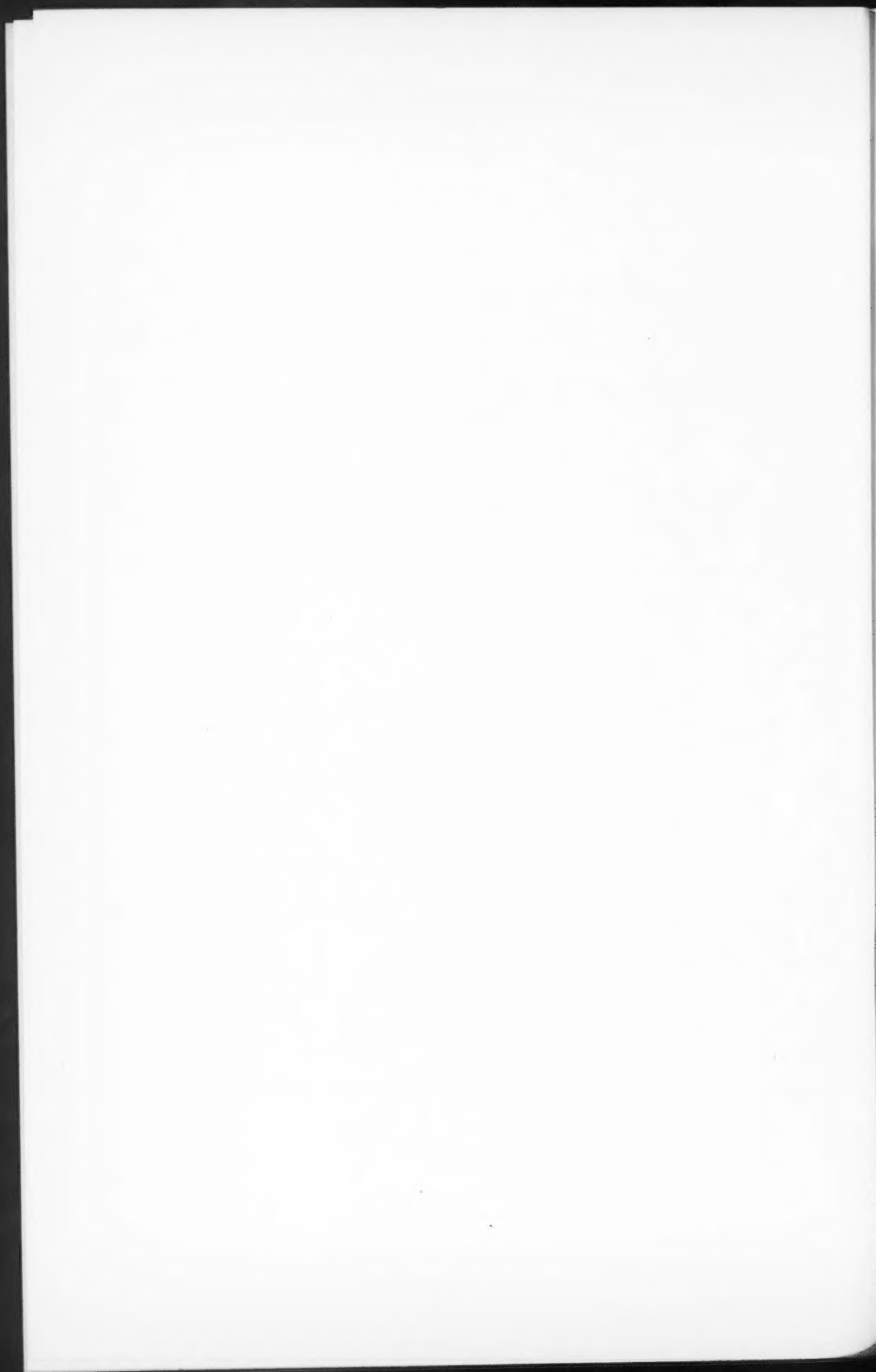


FIG. 1. Two sequences ($\Delta v = 0$ and $\Delta v = 1$) of the $3\Pi - 3\Pi$ band system of the BN molecule.
 FIG. 2. Fine structure of the 0-0 band of the $3\Pi - 3\Pi$ bands of BN.



will be remembered that the conclusion that BN is the emitter of the bands is also in agreement with the experimental conditions for their production.

A formula of the usual type to represent the bands of $B^{11}N$ is easily evaluated from the data of Table I. It is

$$\nu_H = 27775.8 + (1302.6 \nu' - (14.9 \nu'^2) - (1502.3 \nu'' - 12.3 \nu''^2))$$

Rotational Structure of the Triplet System

Fig. 2 gives as an illustration an enlarged spectrogram of the 0-0 band of the triplet system. It is seen that there is a series of groups of five lines (apart from considerably weaker lines) of which four fall into two pairs and the fifth one has about double the intensity of the other and therefore is most probably an unresolved doublet similar to the other pairs. The most plausible, and it seems the only possible, explanation of these series of lines is that they represent the *P* branches of a ${}^3\Pi - {}^3\Pi$ transition. As is well known, in such a transition three *P*, three *Q*, and three *R* branches occur, each of which is double because of Λ -type doubling. The *Q* branches are so weak that they are usually not observed. The *R* branches in the present case form the three heads of a band, but unfortunately are not sufficiently well resolved for analysis.

According to the theory, if both states belong to Hund's Case (*a*) the magnitude of the Λ doublet splitting should be smallest for the ${}^3\Pi_2 - {}^3\Pi_2$ component and largest for the ${}^3\Pi_0 - {}^3\Pi_0$ component, whereas for Hund's Case (*b*) the splitting should be about the same for the three components. The observed splittings are intermediate between these two cases. It seems safe to consider the long-wave-length component of each triplet as belonging to ${}^3\Pi_2 - {}^3\Pi_2$, since it appears single in all three bands whose fine structure has been investigated. However it is rather anomalous that in the 1-0 band the short-wave-length components, which accordingly belong to ${}^3\Pi_0 - {}^3\Pi_0$, are not resolved into doublets.

The fact that lines with the same *K* value fall fairly close together indicates that the two ${}^3\Pi$ states cannot be very far from Hund's Case (*b*).

In the 0-0 band a group of weaker lines accompanies each of the groups of stronger lines. These weaker groups are very similar in structure to the stronger ones and were at first thought to form the returning part of the *R*-branch. However, a closer examination showed that the weaker branch does not run parallel to the strong one as it should if it were the *R* branch. Its spacing is indeed in agreement with the assumption that it is the *P* branch of the isotopic $B^{10}N$ 0-0 band. Thus, since the *R* branches are not resolved it is impossible to carry out the rotational analysis in the usual fashion by means of the combination differences $\Delta_2 F(J)$. Yet on account of the observation of the *P* branches in three bands it is possible to determine the rotational constants by another, though rather more complicated and less accurate, procedure.

TABLE II

Wave numbers of the lines of the P branches of the $^2\Pi-^3\Pi$ B 14 N bands.

J	0-0 band			1-0 band			0-1 band		
	$^2\Pi_2-^3\Pi_2$	$^2\Pi_1-^3\Pi_1$	$^2\Pi_0-^3\Pi_0$	$^2\Pi_2-^3\Pi_2$	$^2\Pi_1-^3\Pi_1$	$^2\Pi_0-^3\Pi_0$	$^2\Pi_2-^3\Pi_2$	$^2\Pi_1-^3\Pi_1$	$^2\Pi_0-^3\Pi_0$
7	27711.92			29002.94			26219.54		
8	07.31			28997.95	29007.09 06.57	29015.59	15.24	26223.49	
9	02.49	27711.02		92.67	01.93 01.42	10.21	10.77	18.79	
10	27697.39	06.55 05.97	27714.51	87.13	28996.44 95.97	Overlapped	06.09	14.17	26227.07 26.52
11	92.15	01.32 00.71	10.18 09.21	81.36	90.78 90.31	28999.06	01.27	09.29	22.29 21.71
12	86.64	27695.86 95.24	04.65 03.72	75.38	84.87 84.36	93.20	26196.32	04.33	17.40 16.81
13	80.90	90.19 89.55	27698.96 98.11	69.05	78.67 78.17	Overlapped	91.15	26199.14	12.31 11.73
14	75.09	84.33 83.73	93.07 Overlapped	62.72	72.30 71.79	80.74	85.77	93.83	01.80 Overlapped
15	69.00	78.31 77.71	Overlapped Overlapped	55.92	Overlapped Overlapped	74.16	Overlapped	88.34	Overlapped 26195.77
16	62.70	72.06 71.15	Overlapped 80.02	48.95	58.78 58.23	Overlapped	Overlapped	82.68	90.80 90.17
17	56.16	65.61 65.02	74.43 73.70	41.72	51.70 51.20	60.27	68.76	76.86	84.92 84.42
18	49.44	58.95 58.36	67.77 67.11	34.25	44.26 43.78	53.75	62.69	70.91	79.01 78.48
19	42.51	52.15 51.58	61.02 60.34	26.52	36.48	45.88	56.56	64.77	Overlapped Overlapped
20	35.36	45.09 44.54	54.09 53.42	18.53	28.67	38.18	50.21	58.49	66.68 66.17
21	28.05	37.83 37.30	46.89 46.30	10.35	20.59	30.27	43.68	52.04	60.61 59.85
22	20.50	30.42 29.89	39.50 38.96	01.96	12.30	22.10	36.97	45.44	53.78 53.18
23	12.78	22.80 22.26	32.01 31.48	28893.26	03.83	13.71	30.22	38.64	47.09 46.60
24	04.83	14.96 14.44	24.29 23.79	84.34	28895.01	05.13	23.13	31.69	40.21 39.76
25	27596.69	06.95 06.43	16.37 15.91	75.15	86.00	28896.27	15.88	24.65	33.29 32.71
26	88.29	27598.69 98.19	08.24 07.83	65.74	76.79	87.17			
27	79.74	90.27 89.81	27599.93 99.55						
28		81.60 81.19	91.44 91.11						

Since for the average of the lines of equal values of J in a ${}^3\Pi-{}^3\Pi$ band the same formulae hold as for a ${}^1\Sigma-{}^1\Sigma$ transition [see Budó (1,2)], these averages were used in the further calculations.* Quadratic formulae of the type

$$(1) \quad \nu = a + bm + cm^2$$

were then fitted to these averaged P branches of the three bands 0-0, 1-0, and 0-1 whose fine structure could be measured. Since

$$(2) \quad P(J) = \nu_0 - (B' + B'')J + (B' - B'')J^2$$

it would be possible to calculate for each band B' and B'' from the coefficient b and c in the empirical equation (1) if $m = -J$,—that is if the correct numbering were known. In this way one should obtain the same B' for the 0-0 and 0-1 bands and the same B'' for the 0-0 and 1-0 bands. Conversely the correct numbering can be found by trying various numberings and determining in every case B' and B'' for each band. With sufficiently accurate data only one numbering will give agreement of the B' and B'' values respectively for the pairs of bands given above. This was in fact found to be the case. The numbering thus determined is used in Table II, which gives the wave numbers of the observed lines of the P branches of the three bands.

It may be mentioned that the two numberings, different by ± 1 unit from the one finally adopted, apart from giving poorer agreement for B' and B'' respectively also would have led to negative values for the rotational constant α .

TABLE III
ROTATIONAL CONSTANTS

ν	Upper state (${}^3\Pi$)		Lower state (${}^3\Pi$)	
	B_v' , cm. ⁻¹	D' , cm. ⁻¹	B_v'' , cm. ⁻¹	D'' , cm. ⁻¹
0	1.550	(8.7·10 ⁻⁶)*	1.654	(8.1·10 ⁻⁶)*
1	1.540		1.629	

* The D value were calculated from the formula $D = \frac{4B^3}{\omega^2}$.

The final rotational constants B_v' and B_v'' which were corrected for the influence of the centrifugal stretching (rotational constant D) are given in Table III. From them B_e' , B_e'' , α_e' , α_e'' , the moments of inertia, and the internuclear distances were evaluated. These data are collected together with the vibrational constants in Table IV.

As mentioned before, the ${}^3\Pi-{}^3\Pi$ BN bands are very probably the analogue of the ${}^3\Pi_g-{}^3\Pi_u$ Swan bands of the C_2 molecule, which has the same number of electrons as BN. For C_2 most of the evidence points to the conclusion that the lower state ${}^3\Pi_u$ of the Swan bands is the ground state. It is therefore probable, although not certain, that the lower state of the ${}^3\Pi-{}^3\Pi$ BN

* It should be noted that lines of one group have the same value of K but different value of J . Thus the averages have to be taken between appropriate lines of three successive groups (see Table I).

TABLE IV
MOLECULAR CONSTANTS OF $B^{11}N$ IN THE UPPER AND LOWER STATE
OF THE TRIPLET BANDS*

	Upper state ($^3\Pi$)	Lower state ($^3\Pi$)
B_e , cm^{-1}	1.555	1.666
α_e , cm^{-1}	0.010	0.025
I_e , gm.-cm^2	$18.00 \cdot 10^{-40}$	$16.80 \cdot 10^{-40}$
r_e , $\text{cm}.$	$1.326 \cdot 10^{-8}$	$1.281 \cdot 10^{-8}$
r_0 , $\text{cm}.$	$1.328 \cdot 10^{-8}$	$1.286 \cdot 10^{-8}$
ω_e , cm^{-1}	1317.5	1514.6
ω_0 , cm^{-1}	1302.6	1502.3
$\omega_e x_e = \omega_0 x_0$, cm^{-1}	14.9	12.3
A_0 (excitation energy)**, cm^{-1}	27775.8	0

* These data although given to the same number of decimal places are not quite as accurate as those for B_2 (4).

** This refers to the head of the 0-0 band. The wave number of the origin of this band which corresponds to the excitation from $J'' = 0$ to $J' = 0$ is about 25 cm^{-1} smaller.

bands is the ground state of the BN molecule. In this connection it is interesting to compare some of the data for the $^3\Pi_u$ state of C_2 with those of the lower state of the BN bands. For C_2 [see Herzberg (5)] $r_e = 1.3121 \cdot 10^{-8} \text{ cm}.$, $\omega_e = 1641.70 \text{ cm}^{-1}$. Both these values are slightly larger than those of BN but of a very similar magnitude. For the upper state the difference between the data for C_2 and BN is larger [$r_e'(C_2) = 1.265$, $\omega_e'(C_2) = 1792.6$].

The Singlet System

Under the same conditions as the above-described triplet system, three further bands were observed with their main heads at

$$30963.3, 32817.2, \text{ and } 34498.8 \text{ cm}^{-1}$$

The first band is shaded to the violet, the last two are to the red. In addition each has a weaker head at

$$30985.4, 32838.7 \text{ and } 34521.5 \text{ cm}^{-1},$$

respectively, the first of which is very weak.

The two long-wave-length bands show simple branches (the third band is overlapped by a BCI band) which suggest rather definitely that the bands are singlet bands. At first sight the band at 30963.3 cm^{-1} seems to consist of a simple P , Q , and R branch ($^1\Pi - ^1\Sigma$ transition). However the R branch does not form the continuation of the P branch. This may be due to perturbation of the upper rotational levels with low J values. Since for the other two bands which could serve to check this assumption, the head forming R branch is not well resolved, we have not been able to obtain a satisfactory analysis.

At the present stage it is impossible to decide definitely whether the bands belong to one and the same band system. If they do they would have to be interpreted as 0-1, 0-0, and 1-0 bands respectively. This interpretation

would lead to $\Delta G_{\frac{1}{2}}' = 1681.6$ and $\Delta G_{\frac{1}{2}}'' = 1853.9$, values which are rather high though not impossibly high. The two heads for the two short-wave-length bands would then be interpreted as *R* and *Q* heads, whereas the very weak second head in the 0-1 band (which is best resolved) would have to be interpreted as the head of the corresponding $B^{10}N$ band (the *P* branch in this band does not come to a head; the strong observed head is a *Q* head). The fact that the 0-1 band is shaded to the red whereas the other two are shaded to the violet is no reason against assigning them to the same band system as the cases of N_2^+ and CN show [see (5)]. Indeed the fact that in the 0-1 band the *P* branch does not come to a head shows that *B'* is only slightly larger than *B''*, whereas for the other two bands *B'* is not very much smaller than *B''*, as indicated by the comparatively large separation of the *P* and *Q* heads.

Because of overlapping by other bands when the exposure time is increased it will not be easy to arrive at a definite decision as to the interpretation of the singlet bands with the method of excitation used here.

Acknowledgments

We are greatly indebted to the American Philosophical Society for a grant from the Penrose Fund, through which the grating spectrograph was provided.

References

1. BUDÓ, A. Z. Physik. 96 : 219-229. 1935.
2. BUDÓ, A. Z. Physik. 98 : 437-444. 1936.
3. DOUGLAS, A. E. and HERZBERG, G. Phys. Rev. 57 : 752. 1940.
4. DOUGLAS, A. E. and HERZBERG, G. Can. J. Research, A, 18 : 165-174. 1940.
5. HERZBERG, G. Molecular spectra and molecular structure. I. Diatomic molecules. Prentice-Hall, Inc., New York. 1939.
6. MULLIKEN, R. S. Phys. Rev. 25 : 259-294. 1925.

COLLIMATED LIGHT BEAMS IN SPECTROPHOTOMETRY¹BY G. O. LANGSTROTH², W. W. BROWN,³ AND K. B. NEWBOUND³

Abstract

Theoretical analysis has predicted that considerable variation is permissible in the distance between the linear light source (a slit) and the "collimating" lens comprising a commonly used spectrophotometric system. This prediction has been tested experimentally over a wide range of source-to-lens distances. The results are in accord with the theoretical expectation.

An optical system commonly used in spectrophotometry consists of a line source of light (e.g., a slit), a collimating lens, and an absorption cell containing the solution to be investigated. For such a system the relation between the optical density of the solution and the transmission is expected to differ from the Lambert-Beer relation by a multiplicative factor (2). This factor does not reduce to unity when the source is placed at the principal focus of the lens, but in general the departure from unity is small. That the magnitude of the factor is only slightly affected by markedly increasing the lens-to-source distance is a prediction of some importance from the viewpoint of instrument design. The present article describes an investigation designed to test this leading feature. The results obtained are in accordance with the theoretical expectations.

Experimental Procedure

The apparatus is shown diagrammatically in Fig. 1. It permitted an investigation of changes in the measured transmission of a solution as the distance between the light source (a slit) and collimating lens was varied. The term "transmission" signifies the ratio of the intensity transmitted through the cell containing the solution to that transmitted through an identical cell containing the solvent.

An image of a 32 volt, 100 watt inside frosted tungsten lamp, U , was formed by means of a lens, M , on a screen containing a slit, S . The light passed through a compensating cell, W or W' , and through a red glass filter, F . Light from the slit was received by the collimating lens, L , whose aperture was limited by a circular diaphragm, D ; it then passed through an absorption cell, C or C' , and was incident finally on a barrier layer photocell, P . The compensating cell W and the absorption cell C contained aqueous copper sulphate solution, while the cells W' and C' contained distilled water. Sliding mounts permitted either of the compensating cells or either of the absorption cells to be inserted in the light beam. The collimating lens, absorption cells, and photocell were mounted on a single base and could be moved as a unit

¹ Manuscript received October 24, 1940.

Contribution from the Physics Department, University of Manitoba, Winnipeg, Man.

² Associate Professor of Physics.

³ Holders of bursaries under the National Research Council of Canada.

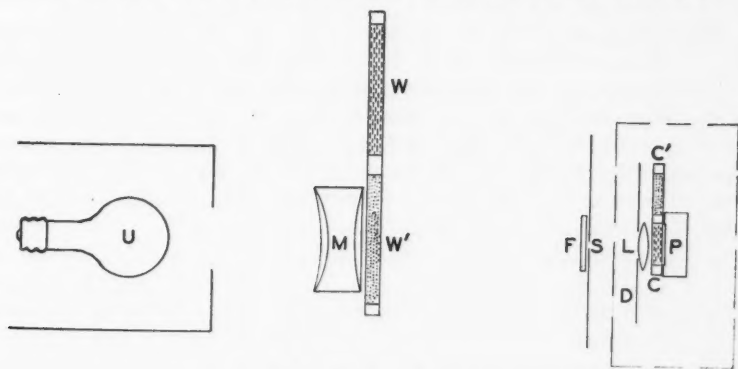


FIG. 1. Diagram of apparatus.

along the optic axis of the system. All other components of the system were fixed.

The following procedure was adopted in making a measurement. The collimating lens was fixed at a given distance from the slit. The galvanometer deflection was noted with compensating cell W' and absorption cell C in the light beam. Cells W and C' were then inserted and the deflection was again noted. The deflections were converted into terms of energy incident on the photocell by means of a calibration curve (Fig. 2). The ratio of these energies was proportional to the transmission of the copper sulphate solution. This procedure was repeated with the collimating lens at various distances from the slit; the range covered extended from one to three or four times the focal length of the lens (Cf. Tables I to III).

The lamp, U , was operated from a double bank of storage batteries. After a preliminary running period, repeated checks of the photocell response over a half-hour interval showed no variations that could not be attributed to experimental error in reading galvanometer deflections. The condensing doublet, M , had a 10 cm. diameter and a 10 cm. effective focal length. These characteristics were required in order that the lamp image should extend beyond the ends of the slit and that the diverging ray bundle should completely fill the collimating lens at all times. Characteristics of the filter, F , are given in Fig. 3. The slit was 3.4 cm. long and 1 mm. wide. The "Photronic" cell, P , was connected to a galvanometer of sensitivity 2.2×10^{-9} amp. per mm. The internal depths of the compensating and absorption cells were respectively 0.83 and 0.68 cm.

Investigations were carried out with two different lenses, (a) a 5 cm. f 1.25 lens and (b) a 10 cm. f 2.5 lens. Lenses of high light-gathering power were chosen since according to the theoretical analysis they are associated with more marked changes in the transmission value on altering the slit-to-lens distance. For a similar reason a high concentration of copper sulphate was used in the absorption cell, viz. 1.0 M .; this solution transmitted about

2% of the filtered light incident upon it. The concentration of the copper sulphate in the compensating cell, W , was adjusted so that approximately equal deflections were obtained when, W , and, C' , were substituted for W' , and, C . This was done for the following reasons: (a) in order that both deflections should be sufficiently large for accurate reading; (b) to obviate calibration of the photocell-galvanometer system over a wide range of incident intensity; and (c) to ensure that the wave-length distribution of the light on the photocell remained essentially constant.

The relation between galvanometer deflection and energy incident on the photocell was determined for the wave-length band used in the experiments with a precision considerably higher than that attained in the actual measurements of transmission. The slit, S , was removed and the condensing doublet, M , was replaced by a 10 cm. f 2.5 lens, whose aperture was varied in a known manner. The calibration curve is shown in Fig. 2.

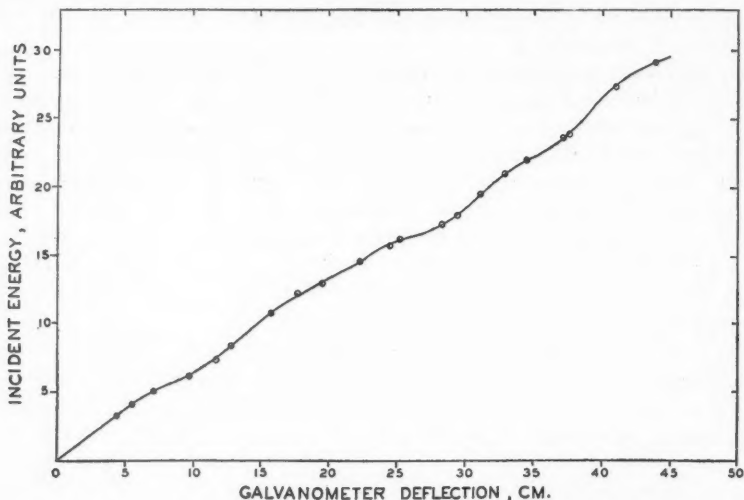


FIG. 2. Relation between galvanometer deflection and light energy incident on the photocell.

Results

Typical results for two lenses of different focal length are given in Tables I and II. Results obtained when light was permitted to pass only through the peripheral portion of the collimating lens are given in Table III. A 1.0 M copper sulphate solution and a slit length of 3.4 cm. were used throughout the experiments.

The values given in the second column of each table represent the averages of two sets of observations. They were obtained by multiplying the determined ratios of the energies incident on the photocell by 0.02; this corrected for the effect of the compensating cell, which transmitted about 2% of the

incident light. Accordingly, the absolute values of the transmission are approximate, but the relative values are good to better than 0.4%. The third column of each table gives the percentage change in the transmission.

Calculated values for the percentage change in transmission are given in the fourth column of each table. The following considerations enter into the calculations. For monochromatic light, the transmission T_λ is given (2) by

$$T_\lambda = e^{-d}(1 - Kd) \quad (1)$$

where

$$K = \frac{1}{2n^2p^2} \left[\frac{H^2}{3} + \frac{(p-f)^2(R_2^2 + R_1^2)}{2f^2} \right] \quad (1a)$$

The symbols d and n denote respectively the optical density and refractive index of the solution, p represents the slit-to-lens distance, $2H$ the length of the slit, and f and R_2 the focal length and radius of the collimating lens. R_1 denotes the radius of an opaque disc centrally placed on the collimating lens (cf. Table III); for the conditions of Tables I and II, R_1 has zero value. For a wave-length band of finite width the effective transmission T_{eff} is given by the ratio of the transmitted energy to the incident energy, each being summed over the band. It follows that

$$T_{eff} = \frac{\sum_\lambda T_\lambda \phi(\lambda)}{\sum_\lambda \phi(\lambda)}, \quad (2)$$

where $\phi(\lambda)$ represents the energy-wave-length distribution of the incident light. Over a wave-length range such that changes in f and n are small, K is independent of λ . Hence,

$$T_{eff} = \frac{\sum_\lambda e^{-d} \phi(\lambda)}{\sum_\lambda \phi(\lambda)} - \frac{K \sum_\lambda d e^{-d} \phi(\lambda)}{\sum_\lambda \phi(\lambda)}. \quad (3)$$

The first term represents the transmission expected on the basis of the Lambert-Beer law; the second term is a relatively small correction factor introduced by the failure of the optical system to collimate perfectly the light passing through the absorption cell. The percentage change in transmission associated with a change Δp in the source-to-lens distance, and a corresponding change ΔK in K is very nearly

$$100 \Delta K \frac{\sum_\lambda d e^{-d} \phi(\lambda)}{\sum_\lambda e^{-d} \phi(\lambda)}. \quad (4)$$

Since the corresponding expression for monochromatic light is $100 \Delta K d$, it is apparent that the changes in transmission with p occur in the same way whether monochromatic light or a wave-length band of finite width is used.

An effective value for $\sum_\lambda e^{-d} \phi(\lambda)$ was determined by summing graphically over the range 6000 to 6800 Å the product of the ordinates of the curves for lamp emission, filter transmission, photocell response, and copper sulphate transmission (Fig. 3). In a similar way, a value for $\sum_\lambda d e^{-d} \phi(\lambda)$ was obtained from the curves mentioned above, together with the optical density curve for the copper sulphate solution. The expected percentage changes in transmission of the copper sulphate solution were then calculated from expression (4). These changes are about 60% of the changes expected for monochromatic light transmitted through a solution of equivalent optical density.

Discussion

The data of Tables I and II show that the observed transmission of the solution varied by less than the experimental error of measurement (0.4%), even though the lens-to-source distance was increased from one to three or four times the focal length of the lens. The data of Table III exhibit a

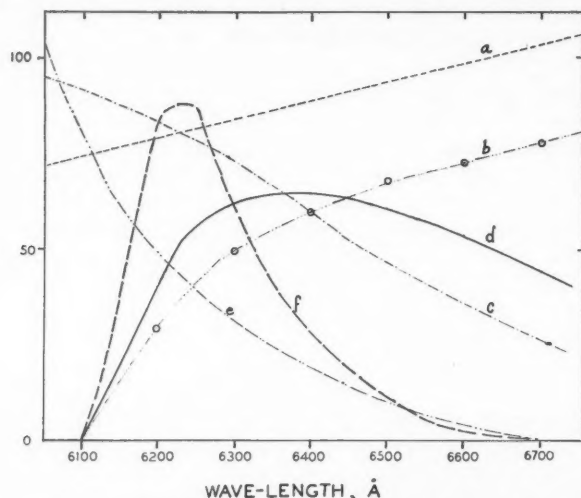


FIG. 3. (a) Energy distribution of radiation emitted by a tungsten filament at 2600° K. [(1, vol. 5, pp. 238-242) together with emission coefficients of tungsten]; (b) determined transmission curve for the filter; (c) sensitivity curve for the photocell (3); (d) 'effective' energy distribution, Φ , of incident light [viz., the products of ordinates of curves a, b, and c]; (e) transmission curve for a 1.0M aqueous copper sulphate solution in a cell of 0.68 cm. depth; (1, vol. 5, p. 330); (f) response curve for the photocell [viz. the products of ordinates of curves d and e]. All ordinates are in arbitrary units. It appears from consideration of curve (f) that about 75% of the photocell response in these experiments was attributable to radiation in the wave-length range 6150 - 6350 Å.

TABLE I

FOCAL LENGTH OF LENS, 10 CM.; APERTURE, 3.2 CM.

Distance from slit to lens p , cm.	Observed transmission, T	Percentage change in transmission	
		Observed	Calculated
10.0	0.01992	-0.4	-0.3
12.0	0.01998	-0.1	-0.1
14.0	0.02000	0.0	0.0
16.0	0.02000	0.0	0.0
18.0	0.02000	0.0	0.0
20.0	0.02000	0.0	0.0
22.0	0.02002	+0.1	0.0
24.0	0.02000	0.0	0.0
26.0	0.02000	0.0	0.0
28.0	0.01998	-0.1	-0.1
30.0	0.01998	-0.1	-0.1

TABLE II
FOCAL LENGTH OF LENS, 5.0 cm.; APERTURE, 3.2 cm.

Distance from slit to lens, p , cm.	Observed transmission, T	Percentage change in transmission	
		Observed	Calculated
5.0	0.02012	-0.5	-0.8
5.5	0.02014	-0.4	-0.4
6.0	0.02020	-0.1	-0.2
6.5	0.02024	+0.1	-0.1
7.0	0.02016	-0.1	0.0
7.5	0.02024	+0.1	0.0
8.0	0.02024	+0.1	0.0
8.5	0.02018	-0.2	0.0
9.0	0.02020	-0.1	0.0
9.5	0.02012	-0.5	0.0
10.0	0.02016	-0.3	0.0
10.5	0.02024	+0.1	0.0
11.0	0.02024	+0.1	0.0
11.5	0.02020	-0.1	0.0
12.0	0.02016	-0.3	-0.1
12.5	0.02016	-0.3	-0.1
13.0	0.02014	-0.4	-0.2
13.5	0.02028	+0.3	-0.2
14.0	0.02026	+0.2	-0.2
14.5	0.02020	-0.1	-0.3
15.0	0.02018	-0.2	-0.3
15.5	0.02018	-0.2	-0.3
16.0	0.02022	0.0	-0.4
17.0	0.02020	-0.1	-0.4
18.0	0.02016	-0.3	-0.5
19.0	0.02016	-0.3	-0.5
20.0	0.02014	-0.4	-0.6

TABLE III
FOCAL LENGTH OF LENS, 5.0 cm.; APERTURE, 3.2 cm.; CENTRAL OPAQUE STOP OF 2.2 cm. DIAMETER

Distance from slit to lens, p , cm.	Observed transmission, T	Percentage change in transmission	
		Observed	Calculated
5.0	0.02008	-0.2	-1.0
5.5	0.02000	-0.6	-0.6
6.0	0.02000	-0.6	-0.2
6.5	0.02000	-0.6	-0.1
7.0	0.02008	-0.2	0.0
7.5	0.02012	0.0	0.0
8.0	0.02010	-0.1	0.0
8.5	0.02012	0.0	0.0
9.0	0.02014	+0.1	-0.1
9.5	0.02010	-0.1	-0.1
10.0	0.02018	+0.3	-0.2
10.5	0.02004	-0.4	-0.2
11.0	0.02000	+0.4	-0.3
11.5	0.01992	-1.0	-0.4
12.0	0.02000	-0.6	-0.5
13.0	0.01994	-0.9	-0.6
14.0	0.01988	-1.2	-0.7
15.0	0.01988	-1.2	-0.9
16.0	0.01992	-1.0	-1.0
17.0	0.01982	-1.5	-1.1
19.0	0.01980	-1.6	-1.3
20.0	0.01986	-1.3	-1.4

detectable variation in the transmission; the trend is in the direction expected from theoretical considerations. While an accurate check of individual calculated values has not been practical because of the high precision of measurement required, the data furnish strong support for the chief prediction of the theory, viz., that with the optical system described, the source of light may be placed at a considerable distance from the principal focus of the collimating lens without introducing serious errors in determined transmission values.

References

1. INTERNATIONAL CRITICAL TABLES. McGraw-Hill Book Co., New York. 1929.
2. LANGSTROTH, G. O. J. Optical Soc. Am., 29 : 381-386. 1939.
3. WESTON ELECTRICAL INSTRUMENTS CORP. Technical data sheet. 1938.

CANADIAN JOURNAL OF RESEARCH

VOLUME 18

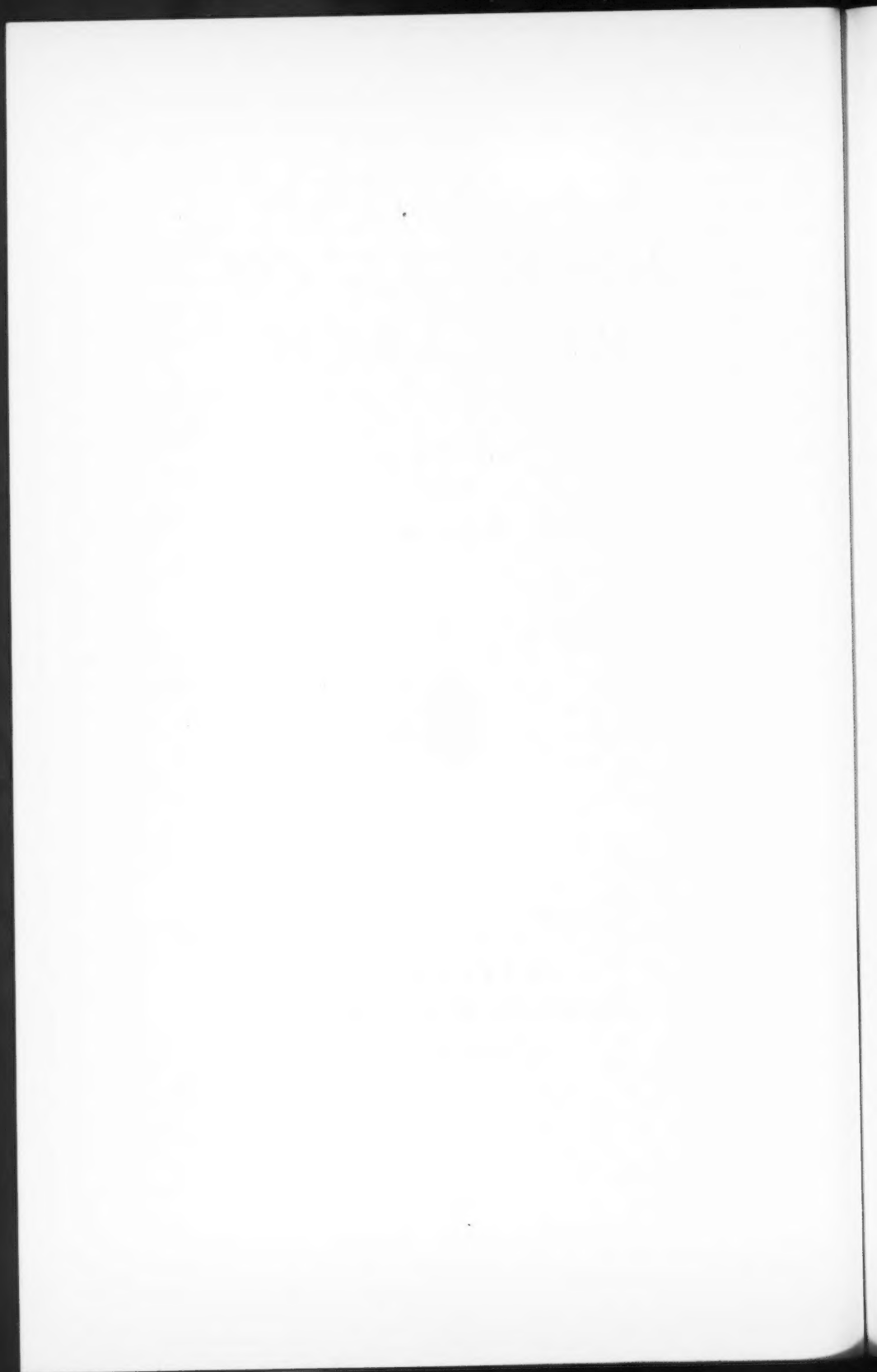
1940

SECTION A



CANADA

Published by the
NATIONAL
RESEARCH COUNCIL
of CANADA



Section A

INDEX TO VOLUME 18

Authors

- Allen, F. and Schwartz, M.**—The validity of the Ferry-Porter law in depressed and enhanced states of retinal sensitivity, 151.
- Babbitt, J. D.**—The permeability of building papers to water vapour, 90.
Observations on the permeability of hygroscopic materials to water vapour. I. Observations at relative humidities less than 75%, 105.
- Brown, W. W.**—See Langstroth, G. O.
- Clark, A. L. and Katz, L.**—Resonance method for measuring the ratio of the specific heats of a gas, C_p/C_v . Part I, 23. Part II, 39.
- Cook, W. H. and Steeves, T. A.**—A fluid system for transferring heat over small temperature gradients without forced circulation, 144.
- Douglas, A. E. and Herzberg, G.**—Spectroscopic evidence of the B_2 molecule and determination of its structure, 165.
Band spectrum of the BN molecule, 179.
- Elson, R. G., Smith, H. G., and J. O. Wilhelm.**—The specific heat of manganese from 16° to 22° K., 83.
- Herzberg, G.**—See Douglas, A. E.
- Herzberg, G., Herzberg, L., and Milne, G. G.**—On the spectrum of the P_2 molecule, 139.
- Herzberg, G. and Sutton, R. B.**—Tail bands of the Deslandres-d'Azambuja system of the C_2 molecule, 74.
- Herzberg, L.**—See Herzberg, G.
- Katz, L.**—See Clark, A. L.
- Langstroth, G. O., Brown, W. W., and Newbound, K. B.**—Collimated light beams in spectrophotometry, 186.
- Larose, P.**—A new form of abrasion tester, 161.
- MacKinnon, K. A.**—Radio frequency measurements of ground conductivity in Canada, 123.
- McLeish, C. W.**—Note on a method of plotting electron distribution curves for the F layer, 98.
- Milne, G. G.**—See Herzberg, G.
- Newbound, K. B.**—See Langstroth, G. O.
- Niven, C. D.**—Thermal conductivity of some sedimentary rocks, 132.
- Prebus, A.**—Improved pole piece construction of the objective lens of a magnetic electron microscope, 175.
- Schwartz, M.**—See Allen, F.
- Smith, H. G.**—See Elson, R. G.
- Steeves, T. A.**—See Cook, W. H.
- Sutton, R. B.**—See Herzberg, G.

— II —

Watson, W. H.—On potential momentum and momentum fields in dynamics, 1.

Wilhelm, J. O.—See Elson, R. G.

Wootton, G. A. A recording system designed for the investigation of the electrical relations in the brains of small animals, 65.

SECTION A

INDEX TO VOLUME 18

Subjects

- Abrasion tester**, A new form of, 161.
- Argon**, Ratio of specific heats of, by resonance method, 47.
- Asphalt** saturated building papers, Permeability of, to water vapour, 92.
- Band spectrum** of the BN molecule, 179.
- B₂ molecule**, See Boron molecule.
- BN molecule**, Band spectrum of, 179.
- Boron molecule**, Diatomic, Spectroscopic evidence of, and determination of its structure, 165.
- Boron nitride molecule**, Band spectrum of, 179.
- Brain potential variations** in small animals, Recording system for study of, 65.
- Building papers**, Permeability of, to water vapour, 90.
- Calorimeter** for measurement of specific heats of solids and powdered specimens at liquid hydrogen and helium temperatures, 83.
- Use with manganese, 83.
- Carbon dioxide**, Ratio of specific heats of, by resonance method, 41.
- C₂ molecule**, Tail bands of the Deslandres-d'Azambuja system of the, 74.
- Carbon molecule**, Diatomic, See C₂ molecule.
- Collimated light beams** in spectrophotometry, 186.
- Conductivity**
Ground, Radio frequency measurements of, in Canada, 123.
Thermal, of some sedimentary rocks, 132.
- Deslandres-d'Azambuja system of the C₂ molecule**, Tail bands of the, 74.
- Diatomic boron molecule**, See Boron molecule.
- Diatomic carbon molecule**, See C₂ molecule.
- Diatomic phosphorus molecule**, See Phosphorus molecule.
- Diffusance** of water vapour through building papers, 91.
hygroscopic materials, 105.
- Dynamics**, Potential momentum and momentum fields in, 1.
- Electromotive forces** in brains of small animals, Recording system for study of, 65.
- Electronic structure** of diatomic boron molecule, 172.
- Electron microscope**, Magnetic, Improved pole piece construction of the objective lens of, 175.
- Electron distribution curves** for the F layer, A method of plotting, 98.
- Felts**, Permeability of, to water vapour, 91.
- Ferry-Porter law** in depressed and enhanced states of retinal sensitivity, Validity of, 151.
- Fibreboard**, Transmission of water vapour through, at relative humidities below 75%, 112.
- F layer**, Method of plotting electron distribution curves for the, 98.
- Gas**, Resonance method for determining specific heats of a, 23, 39.
- Ground conductivity in Canada**, Radio frequency measurements of, 123.
- Heat(s)**
Fluid system for transferring, over small temperature gradients, without forced circulation, 144.
Specific
of a gas, Resonance method for measuring ratio of, 23, 39.
of manganese from 16° to 22° K, 83.
- Helium**, Ratio of specific heats of, by resonance method, 48.
- Hydrogen**, Ratio of specific heats of, by resonance method, 45.
- Hygroscopic materials**, Permeability of, to water vapour, 105.
- Kraft papers**, Permeability of, to water vapour, 93.
- Lens**, Objective, of magnetic electron microscope, Improved pole piece construction of, 175.
- Light beams**, Collimated, in spectrophotometry, 186.
- Limestone**, Conductivity of,
bluish grey, 135.
buff, 135.

- Manganese**, Specific heat of, from 16° to 22° K, 83.
- Marble**, Thermal conductivity of,
black, 134.
brown, 134.
white, 134.
- Microscope**, Magnetic electron, Improved pole piece construction of objective lens of, 175.
- Moisture**, Permeability of building papers to, 90.
- Moisture content gradients** through hygroscopic materials, 115.
- Momentum fields and potential momentum in dynamics**, 1.
- Nitrogen**, Ratio of specific heats of, by resonance method, 39.
- Nuclear spin of B¹¹**, 171.
- Optics**
Collimated light beams in spectrophotometry, 186.
- Papers**, Building, Permeability of, to water vapour, 90.
- Permeability of**
building papers to water vapour, 90.
hygroscopic materials to water vapour, 105.
- Phosphorus molecule**, Diatomic, On the band spectrum of the, 139.
- Potential momentum and momentum fields in dynamics**, 1.
- Radio frequency measurements** of ground conductivity in Canada, 123.
- Refrigeration**, Fluid system for transferring heat over small temperature gradients without forced circulation, 144.
- Resonance method for measuring the ratio of the specific heats of a gas**, C_p/C_v , 23, 39.
- Retinal sensitivity**, Validity of the Ferry-Porter law in depressed and enhanced states of, 151.
- Rocks**, Sedimentary, Thermal conductivity of some, 132.
- Sedimentary rocks**, Thermal conductivity of some, 132.
- Sheathing papers**, Permeability of, to water vapour, 91.
- Slate**, Thermal conductivity of, 135.
- Specific heat of manganese** from 16° to 22° K, 83.
- Specific heats of a gas**, Resonance method for measuring ratio of, 23, 39.
- Spectrophotometry**, See Spectroscopy.
- Spectroscopy**
Boron, diatomic molecule, Spectroscopic evidence of, and determination of its structure, 165.
Boron nitride molecule, Band spectrum of, 179.
Carbon, diatomic molecule, Tail bands of the Deslandres-d'Aambuja system of the, 74.
Phosphorus, diatomic molecule, On the band spectrum of the, 139.
- Tail bands of the Deslandres-d'Aambuja system**, 74.
- Tar-saturated building papers**, Permeability of, to water vapour, 93.
- Temperature gradients**, Small, Fluid system for transferring heat over, without forced circulation, 144.
- Tester**, Abrasion, A new form of, 161.
- Textiles**
A new form of abrasion tester, 161.
- Thermal conductivity** of some sedimentary rocks, 132.
- Ultra-violet system of P₂**, Measurement of some bands in, 139.
- Vapour**, Water, Permeability of building papers to, 90.
- Water vapour**, Permeability of building papers to, 90.
hygroscopic materials to, 105.
- Wood**, Transmission of water vapour through, at relative humidities below 75%, 111.

Canadian Journal of Research

Issued by THE NATIONAL RESEARCH COUNCIL OF CANADA

VOL. 18, SEC. B.

DECEMBER, 1940

NUMBER 12

ÉTUDES PHYSICO-CHIMIQUES SUR LES CARBONATES ALCALINS

II. CALCUL DES COEFFICIENTS D'ACTIVITÉ DES CARBONATES DE SODIUM ET DE POTASSIUM, EN SOLUTION AQUEUSE¹

BY LÉON LORTIE² ET PIERRE DEMERS³

Sommaire

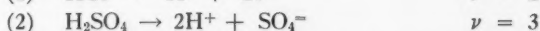
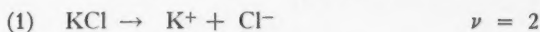
Dans la première partie de ce mémoire, nous décrivons un procédé permettant de calculer, à partir de l'activité du solvant, le coefficient d'activité des ions d'un électrolyte, en tenant compte de la variation, avec la concentration et la température, du nombre ν d'ions par molécule dissoute (hydrolyse, seconde ionisation).

Dans la seconde partie, nous calculons au moyen de ce procédé les coefficients d'activité des carbonates de sodium et de potassium en tenant compte de l'hydrolyse; nous évaluons les erreurs possibles, et nous discutons les résultats obtenus pour les coefficients d'activité des carbonates de lithium, de sodium, et de potassium.

I. Partie théorique

Le procédé habituellement employé pour le calcul des coefficients d'activité des électrolytes forts, et qui est dû à Lewis (13), suppose (i) que l'électrolyte est complètement ionisé à toute concentration, chaque molécule donne naissance à ν ions positifs ou négatifs; (ii) que ν est un nombre entier et constant.

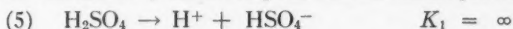
Ainsi en calculant γ pour le chlorure de potassium ou l'acide sulfurique, on écrit:



On calcule aussi avec cette hypothèse, la force ionique de ces solutions. On se rend compte facilement que du choix de ces hypothèses dépend la valeur donnée pour le coefficient moyen γ d'activité des ions:

$$(4) \quad \gamma = (\gamma^{+ \nu} \gamma^{- \nu})^{1/\nu}$$

Ainsi, les valeurs de γ calculées pour l'acide sulfurique en supposant



¹ Manuscrit reçu pour la première fois le 7 mars 1939, et sous forme révisée le 31 juillet 1940. Contribution de l'Institut de Chimie de la Faculté des Sciences de l'Université de Montréal, Montréal, Québec.

Mémoire présenté au congrès de l'American Association for the Advancement of Science Ottawa, Juin 1938.

² Professeur agrégé de chimie générale à la Faculté des Sciences de l'Université de Montréal.

³ Assistant au laboratoire de Physique de la Faculté des Sciences de l'Université de Montréal. Adresse actuelle: 49 Spring Grove Crescent, Outremont, Québec.

* La force ionique μ est définie par l'équation suivante:

$$(3) \quad \mu = \frac{1}{2} \sum_i m_i Z_i^2$$

m_i représente la concentration de l'ion i , en molécules-grammes par 1000g. de solvant; Z_i est la valence de cet ion; la sommation s'étend à tous les ions.

seraient différentes de celles obtenues dans la première hypothèse. Une même solution d'acide sulfurique présente un nombre d'ions ν par molécule globale, une force ionique μ , qui diffèrent dans les deux cas. Si on calcule les coefficients d'activité à partir des points de congélation, la valeur de la fonction auxiliaire j (qui sera définie plus loin) dépend de la valeur assignée à ν ; l'extrapolation de la fonction j jusqu'à $\mu = 0$, est affectée par la valeur de μ .

Le calcul de γ pour les carbonates de sodium et de potassium nous a amenés à établir une formule générale permettant de calculer, à partir de l'activité du solvant, la valeur moyenne de γ pour les ions d'un électrolyte, en supposant une dissociation ionique complète, mais un nombre variable ν d'ions par molécule dissoute.

Nous partons de la formule générale de Gibbs-Duhem qui devient pour un mélange binaire, en introduisant les activités:

$$(7) \quad N_1 d \log a_1 + N_2 d \log a_2 = 0$$

N_1 et N_2 sont les fractions moléculaires, a_1 et a_2 les activités. Pour une solution aqueuse, contenant dans 1000 g. d'eau, m_2, m_3, m_4, m_5 molécules-grammes des molécules ou des ions constituants, cette équation devient:

$$(8) \quad 55.51 d \log a_1 + m_2 d \log a_2 + m_3 d \log a_3 + m_4 d \log a_4 \dots = 0$$

L'activité de l'eau est représentée par a_1 et sa concentration par $m_1 = 55.51$.

Cette équation peut se mettre sous une forme commode dans l'hypothèse d'une ionisation totale: les concentrations des ions, $m_2, m_3, m_4 \dots$ sont simplement proportionnelles à la concentration M , à toute concentration; on tire alors:

$$(9) \quad -55.51 d \log a_1 = \nu M(d \log M + d \log \gamma)$$

en définissant γ par l'équation suivante:

$$(10) \quad \gamma = (\gamma_2^{\nu_2} \cdot \gamma_3^{\nu_3} \cdot \gamma_4^{\nu_4} \dots)^{1/\nu}$$

$\gamma_2, \gamma_3, \gamma_4, \dots$ représentent les coefficients d'activité individuels des ions $\nu_2, \nu_3, \nu_4, \dots$ le nombre d'ions présents par molécule dissoute.

Si, au contraire, la concentration de chaque constituant ionique n'est pas proportionnelle à la concentration M , soit dans le cas d'une ionisation partielle comme pour l'acide sulfurique, ou d'une hydrolyse comme pour le carbonate de sodium, on ne peut obtenir une formule simple et exacte en définissant γ par l'équation précédente. Cependant, si l'on suppose que l'électrolyte est entièrement dissocié en ions, et que les coefficients d'activité de ces ions ont tous la même valeur γ , on tire aisément une équation de même forme que (9):

$$(11) \quad -m_1 d \log a_1 = \nu M(d \log \nu M + d \log \gamma)^*$$

et qui diffère de (9) par les quatre points suivants:

* Si on suppose que l'ionisation de l'électrolyte est partielle, qu'il y a, en plus des ions, des molécules neutres, de concentration m_* , on peut attribuer à ces molécules un coefficient d'activité égal à l'unité, et obtenir les formules suivantes, au lieu de (11) et de (14):

$$(11 \text{ bis}) \quad -m_1 d \log a_1 - \frac{dm_*}{2.3026} = \nu M(d \log \nu M + d \log \gamma)$$

$$(14 \text{ bis}) \quad \log \gamma = -\frac{j}{2.3026} - \int_0^M j d \log \nu M + b \int_0^M \frac{\theta}{\nu M} d\theta - \frac{m_*}{2.3026}$$

1. ν est ici une quantité variable qu'il faut connaître à chaque concentration;

2. Le premier terme de la parenthèse de droite est $d \log \nu M$, au lieu de $d \log M$; ces deux différentielles sont équivalentes si ν est une constante;

3. γ est défini par l'équation (11) elle-même. Nous évaluerons tout à l'heure dans le cas des carbonates alcalins l'écart entre cette valeur trouvée pour γ , et la valeur qu'on obtiendrait en définissant γ comme la moyenne géométrique des coefficients individuels, équation (35);

4. Il faut noter que m_1 n'est exactement égal à 55.51 que dans le cas où l'électrolyte ne réagit pas sur l'eau.

Si on se sert des pressions de vapeur du solvant, on tire facilement:

$$(12) \quad \log \gamma = -\frac{h}{2.3026} - \int_0^M h d \log \nu M$$

La fonction auxiliaire h est définie par:

$$(13) \quad h = \frac{2.3026 m_1 \log a_1}{\nu M} + 1$$

m_1 vaut 55.51, si le solvant est l'eau; ν est calculé pour chaque concentration.

La précision actuelle des mesures de tension de vapeur ne justifierait probablement pas les calculs supplémentaires requis pour cette formule, dans la plupart des cas.

Pour ce qui concerne les mesures de cryométrie, en utilisant l'équation donnée par Lewis et Randall (13) pour exprimer a_1 en fonction de l'abaissement du point de congélation θ , on trouve finalement:

$$(14) \quad \log \gamma_\theta = -\frac{j}{2.3026} - \int_0^M j d \log \nu M + b \int_0^M \frac{\theta}{\nu M} d\theta$$

dans cette équation, ν est une variable fonction de M ou de θ :

$$(15) \quad j = 1 - \frac{\theta}{\nu \lambda M}; \quad b = 0.00025; \quad \lambda = 1.858$$

Si la valeur de ν devient constante, l'équation (14) se ramène à l'équation ordinaire:

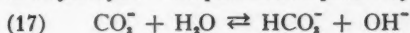
$$(16) \quad \log \gamma_\theta = -\frac{j}{2.3026} - \int_0^M j d \log M + \frac{b}{\nu} \int_0^M \frac{\theta}{M} d\theta$$

II. Application aux carbonates de sodium et de potassium

Nous avons appliqué ces procédés aux données que l'on trouve dans la littérature, sur les carbonates de sodium et de potassium.

Des points de congélation ont été mesurés par Jones (11), de Coppet (3, 4), Loomis (14, p. 504; 15), Meyerhoffer (20), Hill et Bacon (9), Caspari (2), et tout récemment par Ender (5).

Calcul de l'hydrolyse. On peut écrire pour l'hydrolyse:



$$(18) \quad [\text{CO}_3^{2-}] = M(1 - y) \text{ et } [\text{HCO}_3^-] = [\text{OH}^-] = My$$

$$(19) \quad K_{hydr.} = \frac{My^2}{1-y} \cdot \frac{\gamma_{\text{HCO}_3^-} \cdot \gamma_{\text{OH}^-}}{\gamma_{\text{CO}_3^{2-}}}$$

y est le degré, et $K_{hydr.}$, la constante d'hydrolyse; le nombre d'ions par molécule du sel est accru par suite de l'hydrolyse et devient:

$$(20) \quad \nu = 3 + y$$

La force ionique est au contraire diminuée et devient:

$$(21) \quad \mu = M(3 - y)$$

Pour calculer y , il est nécessaire de connaître $K_{hydr.}$ à la température de congélation, qui est comprise entre 0° C. et -40° C.; $K_{hydr.}$ est égale au quotient de K_w , la constante d'ionisation de l'eau par K_2 , la seconde constante de dissociation de l'acide carbonique:

$$(22) \quad K_{hydr.} = \frac{K_w}{K_2}$$

Nous avons calculé K_w en extrapolant les résultats de Harned et Hamer (8) au moyen de la formule qui leur a servi à exprimer K_w entre 0° C. et +60° C. Nous avons tiré K_2 des résultats de MacInnes et Belcher pour 25° C. (16) et pour 38° C. (17), en admettant que la variation de K_2 avec la température suit la loi empirique universelle au moyen de laquelle Harned et Embree (7) représentent le changement des constantes d'ionisation avec la température.

TABLEAU I

K_w = constante d'ionisation de l'eau. K_2 = seconde constante d'ionisation de l'acide carbonique. $K_{hydr.}$ = constante d'hydrolyse de l'ion CO_3^{2-} .

T, ° C.	$10^{16} K_w$	$10^{11} K_2$	$10^5 K_{hydr.}$
0	11.5	4.08	2.82
-10	4.15	3.45	1.203
-20	1.325	2.85	0.465
-30	0.3741	2.33	0.161

La loi d'hydrolyse peut maintenant s'écrire:

$$(23) \quad \frac{K_w}{K_2} = \frac{My^2}{(1-y)} \left(\frac{\gamma_{\text{HCO}_3^-} \cdot \gamma_{\text{OH}^-}}{\gamma_{\text{CO}_3^{2-}}} \right) = \frac{My^2}{(1-y)} \Gamma$$

On ne possède pas de renseignement direct sur Γ .

Si nous écrivons que tous les ions présents ont le même coefficient d'activité γ_θ , comme nous l'avons supposé pour obtenir la formule (14), l'équation précédente est simplifiée, et devient, au point de congélation:

$$(24) \quad \frac{K_w}{K_2} = \frac{My^2}{(1-y)} \cdot \gamma_\theta$$

Remarquons dès maintenant qu'en prenant la dérivée logarithmique de (23), on peut écrire, en négligeant y devant l'unité:

$$(25) \quad \frac{dy}{y} = -\frac{1}{2} \frac{d\Gamma}{\Gamma}$$

Dans nos calculs, y est de l'ordre de 0.06. Une erreur de 10% sur Γ entraîne une erreur de 0.003 sur y . Nous verrons plus loin l'influence de ce résultat dans le calcul final de γ .

Il faut connaître y pour calculer γ , et connaître γ pour calculer y . Nous procédons par approximations successives.

Au moyen de (16), en posant $y = 0$, nous calculons les coefficients d'activité au point de congélation γ_θ , pour les carbonates de sodium et de potassium. Ces résultats sont valables en première approximation. Nous introduisons ces valeurs de γ_θ dans (24), ce qui nous donne une première série de nombres pour y .

Nous pouvons maintenant tenir compte de l'hydrolyse, dans un second calcul de γ_θ , grâce aux formules (20), (21), et (14), et calculer de nouvelles valeurs de y , qui diffèrent peu des précédentes.

Calcul du coefficient d'activité à la température de congélation γ_θ

Une troisième approximation fournit, pour chacun des deux sels, des valeurs suffisamment précises de y (Tableaux III et IV). Avec ces valeurs de y , nous avons calculé pour les points expérimentaux les valeurs de μ et j , d'après les équations (21) et (15). Nous devons représenter j en fonction de $\mu^{\frac{1}{2}}$ sur un graphique à grande échelle. Nous avons tracé une courbe, d'après ces points expérimentaux, en accordant un poids plus grand aux résultats de Ender qui paraissent plus précis que ceux des expérimentateurs précédents. Sur cette courbe, nous avons interpolé, pour des concentrations simples, les valeurs finales de j , qui nous ont servi dans les calculs ultérieurs, effectués par des méthodes semi-graphiques.

Il faut extrapoler les courbes représentant j en fonction de $\mu^{\frac{1}{2}}$ jusqu'à la force ionique 0. En tenant compte de l'hydrolyse, on peut le faire de façon beaucoup plus satisfaisante que lorsqu'on la néglige (Fig. 1: points inférieurs sans correction; courbe supérieure, corrigée). Les mesures de Ender semblent donc assez précises pour justifier le sens et l'ordre de grandeur de la correction due à l'hydrolyse. Un procédé destiné à en tenir compte vaut donc la peine d'être appliqué.

En supposant une loi limite linéaire, on a:

$$(26) \quad j = \beta \mu^{\frac{1}{2}}$$

$\beta = 0.534$ pour le carbonate de sodium; $\beta = 0.509$ pour le carbonate de potassium.

Pour calculer γ_θ à la concentration de 0.005 M , nous avons supposé que la variation de j en fonction de $\mu^{\frac{1}{2}}$, dans une solution du carbonate non-dissocié, suivrait cette loi. L'hypothèse parut plausible, car cette loi limite est déduite

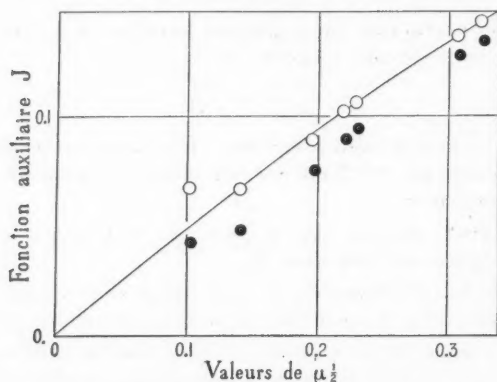


FIG. 1. Variation de la fonction auxiliaire j en fonction de $\mu^{1/2}$. La courbe passe par les cercles représentant les valeurs calculées d'après les points expérimentaux de Ender et corrigées pour tenir compte de l'hydrolyse. Les points noirs situés au-dessous de la courbe ont été calculés sans tenir compte de l'hydrolyse.

de mesures portant sur des solutions où l'hydrolyse de l'ion carbonate ne dépasse pas 10%. On obtient alors pour γ_θ :

$$(27) \quad \log \gamma = -\alpha \mu^{1/2} \quad (M < 0.005)$$

$\alpha = 0.696$ pour le carbonate de sodium; $\alpha = 0.663$ pour le carbonate de potassium.

Pour les concentrations supérieures, les intégrales ont été évaluées graphiquement.

Calculs d'erreurs

Nous allons examiner deux causes d'erreur qui peuvent affecter nos calculs.

1. Examinons d'abord l'effet provenant d'une erreur possible sur la valeur de Γ . Nous avons déjà trouvé:

$$(28) \quad \frac{dy}{y} = -\frac{1}{2} \cdot \frac{d\Gamma}{\Gamma}$$

On peut trouver aussi simplement:

$$(29) \quad dv = dy; \quad d\mu = -M \cdot dy; \quad dj = \frac{\theta}{\nu\lambda M} \cdot \frac{dy}{3+y}$$

Dans la dernière équation on peut négliger, au dénominateur, y vis-à-vis de 3 et écrire:

$$(30) \quad dj = \frac{1}{3} \frac{\theta}{\nu\lambda M} \cdot dy$$

Dérivons l'équation (14) par rapport à y :

$$(31) \quad \frac{d}{dy} (\log_e \gamma_\theta) = -\frac{dj}{dy} - \frac{d}{dy} \int_{M_1}^{M_2} \frac{j}{\nu M} \cdot d(\nu M)$$

Nous négligeons la dérivée du troisième terme du membre de droite de l'équation (14), qui a une valeur très faible. Développons (31):

$$(32) \quad \frac{d \log_e \gamma_\theta}{dy} = -\frac{dj}{dy} - \int_{M_1}^{M_2} \frac{dj}{dy} \cdot \frac{dM}{M} - \int_{M_1}^{M_2} \frac{dj}{dy} \cdot \frac{dv}{v} - \left[\frac{j}{v} \cdot \frac{dv}{dy} \right]_{M_2} + \left[\frac{j}{v} \cdot \frac{dv}{dy} \right]_{M_1}$$

Evaluons cette dérivée entre $M_2 = 0.05$ et $M_1 = 0.005$. $\frac{\theta}{v\lambda M}$ est toujours voisin de 1; $\frac{dj}{dy}$ est donc toujours de l'ordre de 0.33. $v_{0.005} = 308$ et $v_{0.05} = 3.03$. Avec ces indications on peut calculer une limite supérieure de la dérivée:

$$(33) \quad \frac{d \log_e \gamma}{dy} = -0.33(1 + 2.30 + 0.02) = -1.1$$

Les deux derniers termes de (32) sont négligeables. Une valeur de Γ trop élevée de 10% entraîne une erreur de -0.003 sur y , de $+0.003$ sur $\log_e \gamma$ pour la concentration $0.05M$ donc une erreur relative de $+0.3\%$ sur γ . On se rend compte facilement qu'aux concentrations supérieures, l'erreur finale sur γ résultant d'une erreur de 10% sur Γ ne peut guère dépasser 0.5%. Cette erreur paraît donc négligeable. (Cette erreur concerne le rapport $\gamma_M/\gamma_{0.005}$. La valeur de $\gamma_{0.005}$ est déterminée par la loi limite extrapolée (26) d'après les valeurs de j et de $\mu^{\frac{1}{2}}$ sur lesquelles influent les valeurs de Γ . On ne peut évaluer de façon précise l'erreur sur $\gamma_{0.005}$).

2. Le coefficient d'activité que nous avons déterminé dans l'hypothèse de l'égalité des coefficients individuels, grâce à la formule (14) et que nous désignons ici par γ' , n'est pas rigoureusement égal au coefficient moyen d'activité des carbonates de sodium ou de potassium que nous désignerons par γ .

Voici les équations exactes qui définissent γ et γ' ; l'indice 2 se rapporte au cation Na^+ ou K^+ , l'indice 3 à l'ion CO_3^{2-} , l'indice 4 à l'ion OH^- , l'indice 5 à l'ion HCO_3^- :

$$(34) \quad d \log \gamma' = \frac{\nu_2}{\nu} d \log \gamma_2 + \frac{\nu_3}{\nu} d \log \gamma_3 + \frac{\nu_4}{\nu} d \log \gamma_4 + \frac{\nu_5}{\nu} d \log \gamma_5$$

$$(35) \quad \gamma = \gamma_2^{\frac{2}{3}} \gamma_3^{\frac{1}{3}}$$

ou:

$$(36) \quad d \log \gamma = \frac{2}{3} d \log \gamma_2 + \frac{1}{3} d \log \gamma_3$$

Cherchons à évaluer l'écart entre γ et γ' . Tenant compte de la réaction (17), on trouve facilement:

$$(37) \quad \nu = 3 + y; \quad \nu_2 = 2; \quad \nu_3 = 1 - y; \quad \nu_4 = y = \nu_5$$

en retranchant (34) de (36):

$$(38) \quad d \log \frac{\gamma}{\gamma'} = \frac{1}{3} \left(\frac{y}{3+y} d \log \frac{\gamma_2^2 \gamma_3^4}{\gamma_4^3 \gamma_5^3} \right)$$

On voit que si tous les coefficients $\gamma_2, \gamma_3, \gamma_4, \gamma_5$ sont égaux, γ est bien égal à γ' .

On peut écrire, pour le carbonate de sodium:

$$(39) \quad \frac{\gamma_2^2 \gamma_3^4}{\gamma_4^3 \gamma_5^3} = \left(\frac{\gamma_{\text{Na}_2\text{CO}_3}^2}{\gamma_{\text{NaHCO}_3} \cdot \gamma_{\text{NaOH}}} \right)^6$$

En l'absence de données plus précises, nous évaluerons cette dernière expression en faisant quelques hypothèses.

Nous supposons, conformément à la théorie de Debye et Hückel, $\gamma_2 = \gamma_4 = \gamma_5$, et:

$$(40) \quad \log \gamma_2 = -0.5\mu^{\frac{1}{2}}$$

Nous avons trouvé la loi limite approchée:

$$(41) \quad \log \gamma = -0.67\mu^{\frac{1}{2}}$$

d'où l'on tire:

$$(42) \quad \log \gamma_3 = -1.01\mu^{\frac{1}{2}}$$

Dans ces conditions:

$$(43) \quad \log \frac{\gamma}{\gamma'} = \frac{4}{3} \int_0^M \frac{y}{3+y} d \log \frac{\gamma_3}{\gamma_2} = -\frac{4}{3} \int_0^M \frac{y}{3+y} d(0.51\mu^{\frac{1}{2}})$$

Calculons cette expression pour $M = 0.005$. La valeur de $\frac{y}{3+y}$ reste comprise entre 0.25 et 0.025; prenons la valeur moyenne 0.13. Il vient:

$$(44) \quad \log \frac{\gamma}{\gamma'} = -\frac{4}{3} \times 0.13 \times 0.51 \times 0.1209 = -0.011$$

γ est alors inférieur de 2.5% à γ' . Pour les concentrations supérieures la même formule montre que l'écart ne peut guère s'accroître de plus de 0.6%. Cette erreur affecte donc surtout la valeur de $\gamma_{0.005}$ et assez peu les rapports $\frac{\gamma}{\gamma_{0.005}}$, aux concentrations habituelles.

Nous n'appliquerons pas cette correction, qui ne peut être estimée avec précision; signalons simplement qu'elle équivaldrait à multiplier tous les résultats indiqués dans les tableaux IV et V, pour γ_θ et pour $\gamma_{298.1}$, par un facteur compris entre 0.975 et 0.969.

Les équations que nous venons d'établir montrent la possibilité d'un calcul rigoureux de γ pour un électrolyte hydrolysé.

Calcul de $\gamma_{298.1}$

Pour obtenir le coefficient d'activité $\gamma_{298.1}$ à 25° C. ou 298.1K, température usuelle de référence, il faut calculer, par les données thermochimiques, la fonction x de Lewis et Randall (13):

$$(45) \quad x = \log \frac{a_{1298.1}}{a_{1\theta}}$$

Si le nombre ν peut être considéré comme constant dans une solution de concentration déterminée, quelle que soit la température, on tire finalement:

$$(46) \quad \log \frac{\gamma_{298.1}}{\gamma_\theta} = -55.51 \int_0^M \frac{1}{\nu M} dx$$

Ici encore, le nombre ν est sous le signe d'intégration au lieu de le précéder. Si ν varie notablement avec la température, pour une concentration déterminée, il faudrait prendre une valeur de ν intermédiaire entre celles calculées

pour la température de congélation et pour la température finale désirée (298.1° K.) On pourra, comme première approximation, utiliser la moyenne de ces valeurs. S'il y a des cas qui réclament une précision plus grande encore, il sera possible de diviser l'intervalle de température qui sépare la température de congélation de la température finale, en sous-intervalles appropriés, et de calculer pour chacun, la quantité x , une valeur moyenne de ν , et, par une intégrale, le rapport

$$\frac{\gamma_{\text{température supérieure}}}{\gamma_{\text{température inférieure}}}$$

Nous nous sommes contentés ici de prendre pour ν la valeur au point de congélation; la précision des données thermochimiques ne justifierait pas l'emploi de procédés plus élaborés. On calcule x à partir de données thermochimiques:

$$(47) \quad x = -\bar{L}_1 \frac{T'' - T'}{2.303 RT'' T'} + (\bar{C}_{p_1} - \bar{C}_{p_1}^{\circ}) \left(T'' \frac{T'' - T'}{2.303 RT'' T'} - \frac{1}{R} \log \frac{T''}{T'} \right)$$

$T'' = 298.1$ K; T' la température absolue de congélation $= 273.1 - \theta$;

\bar{L}_1 = chaleur interne partielle de l'eau dans la solution, celle de l'eau pure étant prise égale à zero;

\bar{C}_{p_1} = chaleur spécifique partielle de l'eau dans la solution;

$\bar{C}_{p_1}^{\circ}$ = chaleur spécifique partielle de l'eau dans l'eau pure.

Nous avons évalué $(\bar{C}_{p_1} - \bar{C}_{p_1}^{\circ})$, en nous servant des chaleurs spécifiques de Marignac (18, 19), de Rümelin (23) et de Swallow et Alty (24), par un procédé graphique dû à Lewis et Randall. On porte en abscisses la concentration en grammes de sel par grammes de solution et en ordonnées la chaleur spécifique de la solution. On mène une droite tangente à la courbe en un point de concentration donnée; l'abscisse du point de rencontre de cette droite avec l'axe des abscisses est égale à la chaleur spécifique partielle de l'eau pour cette concentration. Le résultat doit être multiplié par 18 pour nous donner la chaleur spécifique partielle moléculaire de l'eau, \bar{C}_{p_1} (Tableau II).

Nous avons calculé les chaleurs différentielles de dilutions à partir des nombres sur la chaleur de dilution contenus dans International Critical Tables (10, vol. 5, p. 203).

L'équation (46) a été intégrée graphiquement. Les valeurs de $\log \frac{\gamma_{298.1}}{\gamma_{\theta}}$ sont portées dans les tableaux III et IV.

Le résultat final de ces opérations est représenté dans les tableaux III et IV, et sur la fig. 2; $\gamma_{298.1}$ est porté en ordonnées et la racine carrée de la force ionique apparente, en abscisses. L'eutectique du carbonate de sodium apparaissant à une concentration assez faible, les données cryométriques ne vont pas au delà de 0.5 M. Nous avons continué la courbe en utilisant au mieux les pressions de vapeur publiées par Perreu en 1935 (21).

L'eutectique du carbonate de potassium n'apparaît que vers 5 M ; ici encore nous avons continué la courbe, au moyen des pressions de vapeur des International Critical Tables (10, vol. 5, p. 299).

TABLEAU II

$(\bar{C}_{p1} - \bar{C}_{p1}^0) =$ CHALEUR SPÉCIFIQUE PARTIELLE DE L'EAU POUR UNE TEMPÉRATURE VOISINE DE 20° C.

M	Calories (Mol. g.) ² (degré)	
	dans Na_2CO_3	dans K_2CO_3
0.1	-0.0125	-0.009
0.2	-0.045	-0.0216
0.3	-0.0774	-0.04
0.4	-0.094	—
0.5	-0.185	-0.0666
1.0		-0.2645
1.5		-0.516
2.0		-0.877
3.0		-1.363
4.0		-1.707
5.0		-1.956

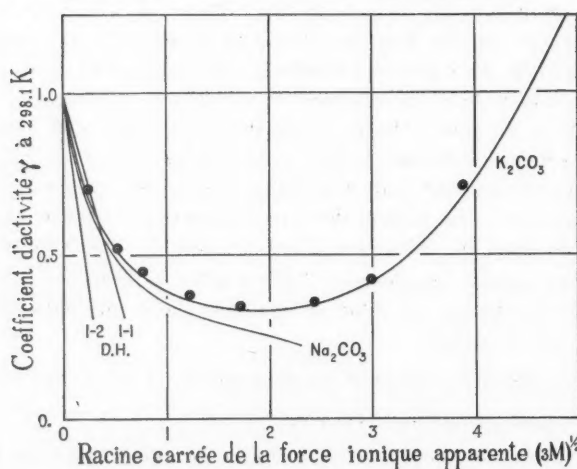


FIG. 2. Valeurs de γ à 25° C. en fonction de $(3M)^{1/2}$, courbes dressées d'après les données cryométriques jusqu'à 0.5 M pour le carbonate de sodium et jusqu'à 5 M pour le carbonate de potassium. Au-delà de ces valeurs, les courbes ont été prolongées en utilisant les données obtenues à partir des pressions de vapeur des solutions. Tous ces points ont été calculés en tenant compte de l'hydrolyse de ces deux sels. La courbe D-H 1-1 est la courbe calculée pour les sels uni-univalents et D-H 1-2, celle des sels bi-univalents. On voit que les courbes des carbonates alcalins se rapprochent de D-H 1-1.

TABLEAU III
CARBONATE DE SODIUM

M	θ , °C.	γ	μ^{\dagger} apparente	μ^{\dagger} corrigée au point de con- gélation	γ_{θ}	$\log \frac{\gamma_{298.1}}{\gamma_{\theta}}$	$\gamma_{298.1}$ cryométrie	$\gamma_{298.1}$ tonométrie
0.005	0.0268	0.0785	0.1225	0.1209	0.8236	0	0.8236	
0.01	0.0517	0.0588	0.1732	0.1715	0.7607	0	0.7607	
0.02	0.0909	0.0445	0.2450	0.2432	0.6814	0	0.6814	
0.03	0.144	0.0382	0.3000	0.2981	0.6294	0	0.6294	
0.05	0.231	0.0308	0.3872	0.3853	0.5621	0	0.5621	
0.1	0.440	0.0241	0.5477	0.5455	0.4720	0.0073	0.4800	
0.2	0.843	0.0186	0.7746	0.7722	0.3891	0.0169	0.4046	
0.3	1.240	0.0162	0.9487	0.9461	0.3462	0.0238	0.3656	
0.4	1.638	0.0147	1.0954	1.0927	0.3185	0.0346	0.3449	
0.463			1.178				(0.334)	(0.334)
0.5	2.036	0.0136	1.2246	1.2218	0.2988	0.0392	0.3270	
0.926			1.668					0.279
1.389			2.041					0.253
1.852			2.357					0.234

TABLEAU IV
CARBONATE DE POTASSIUM

M	θ , °C.	γ , degré d'hydrolyse	μ^{\dagger} apparente	μ^{\dagger} corrigée au point de con- gélation	γ_{θ}	$\log \frac{\gamma_{298.1}}{\gamma_{\theta}}$	$\gamma_{298.1}$ cryomètre	$\gamma_{298.1}$ tonométrie
0.005	0.0268	0.0789	0.1225	0.1209	0.8316	0	0.8316	
0.01	0.052	0.0582	0.1732	0.1715	0.7720	0	0.7720	
0.02	0.101	0.0434	0.2450	0.2432	0.6990	0	0.6990	
0.03	0.147	0.0368	0.3000	0.2982	0.6521	0	0.6521	
0.05	0.236	0.0300	0.3872	0.3853	0.5922	0.0015	0.5943	
0.1	0.457	0.0225	0.5477	0.5457	0.5094	0.0032	0.5132	
0.2	0.885	0.0170	0.7746	0.7724	0.4328	0.0062	0.4390	
0.3	1.310	0.0145	0.9487	0.9464	0.3936	0.0111	0.4038	
0.5	2.180	0.0118	1.2246	1.2222	0.3516	0.0218	0.3697	
1	4.520	0.0076	1.7321	1.7298	0.3143	0.0281	0.3354	
1.5	7.133	0.0050	2.1213	2.1196	0.3069	0.0382	0.3351	(0.3537)
2	10.096	0.0037	2.4495	2.4480	0.3143	0.0485	0.3515	
3	17.635	0.0024	3.0000	2.9988	0.3637	0.0498	0.4079	
3.5			3.240					(0.4314)
4	27.662	0.0013	3.4641	3.4634	0.4622	0.0514	0.5202	
5	39.854	0.0004	3.8730	3.8704	0.6121	0.0603	0.7034	
6			4.243					0.7465
8			4.899					1.2508

Les valeurs de γ seraient plus élevées de quelques centièmes, si nous avions négligé de tenir compte de l'hydrolyse. Les points noirs sur la fig. 2 représentent les résultats que nous aurions obtenus pour le carbonate de potassium au moyen des procédés habituels.

Conclusions

Ces courbes donnent lieu à trois conclusions:

1. La variation de γ en solution diluée rapproche les deux carbonates des sels uni-univalents (Droite D.H. 1-2, sur la fig. 2), plus que des sels bi-univalents (Droite D.H. 1-2, sur la fig. 2). L'hydrolyse, qui donne naissance à des ions univalents, peut expliquer en partie ce résultat. Elle ne peut l'expliquer complètement, car dans les solutions les plus diluées, dont nous avons employé les propriétés cryométriques, l'hydrolyse ne dépasse guère 10%. Cette conclusion s'accorde avec une remarque de MacInnes et Belcher (16, 17).

Ces auteurs expriment leurs résultats expérimentaux par une relation entre pK_2 et la force ionique de leurs solutions, d'où l'on peut tirer une pente limite, pour le carbonate de potassium, à condition d'admettre que, selon la théorie de Debye et Huckel:

$$(48) \quad \log \gamma_{\text{Cl}^-} = \log \gamma_{\text{HCO}_3^-} = \log \gamma_{\text{K}^+} = -0.506 \mu^{\frac{1}{2}}$$

On trouve ainsi une pente limite égale à 1.43 fois la pente limite indiquée par la théorie pour un sel uni-univalent. Celle que nous trouvons est égale à 1.34 fois la pente théorique. Si nous tenons compte de la correction signalée plus haut, qui est due à l'inégalité des coefficients d'activité individuels, la pente devient égale à 1.52 fois la même pente théorique.

2. La courbe du sel de potassium est constamment au-dessus de la courbe du sel de sodium, ce qui assimile les carbonates aux hydroxydes et fluorures; cette remarque a déjà été faite par Ender, qui n'avait cependant pas effectué les calculs numériques. Si l'influence du cation s'exerce dans le même ordre que d'habitude, la courbe du lithium devrait être au-dessus de celle du sodium. Un calcul approché de Brown et Latimer (1) donne la valeur $\gamma = 0.59$ pour une solution saturée de carbonate de lithium à 25° C. Ce résultat placerait la courbe du lithium un peu au-dessus de celle du potassium.

D'autre part, Walker, Bray et Johnston (25) ont indiqué, pour toute une série de forces ioniques, des coefficients d'activité individuels de l'ion CO_3^{2-} , dans des solutions salines contenant du potassium, du sodium ou du lithium. Utilisant leurs nombres et les coefficients individuels donnés pour K^+ , Na^+ , Li^+ par Lewis et Randall (13), nous avons calculé les coefficients d'activité des trois carbonates par la formule:

$$(49) \quad \gamma_{\text{Me}_2\text{CO}_3}^3 = \gamma_{\text{Me}^+}^2 \cdot \gamma_{\text{CO}_3^{2-}}$$

Ces résultats sont représentés dans le tableau V. Les coefficients obtenus se superposent dans l'ordre K, Na, Li et s'accordent à quelques centièmes près avec les calculs que nous avons faits par cryométrie.

TABLEAU V

 γ_1 calculé d'après divers résultats γ_2 interpolé sur notre courbe finale

μ	K		Na		Li
	γ_1	γ_2	γ_1	γ_2	γ_1
0.01	0.83	0.86	0.82	0.86	0.818
0.02	0.78	0.80	0.77	0.79	0.759
0.04	0.72	0.74	0.71	0.73	0.694
0.05	0.70	0.72	0.69	0.71	0.673
0.1	0.62	0.65	0.61	0.62	0.589

3. A force ionique égale, les coefficients d'activité sont compris entre ceux des sulfates et des hydroxydes alcalins. Kielland (12) a publié récemment des tables donnant les coefficients d'activité d'un grand nombre d'ions; les chiffres qu'on peut en tirer pour les carbonates alcalins sont notablement plus faibles que ceux que nous rapportons ici. Redlich et Rosenfeld (22) ont calculé, à partir des données cryométriques des International Critical Tables (10), les coefficients d'activité des carbonates de sodium et de potassium. Ces nombres sont en général plus faibles, de quelques centièmes, que les nôtres.

Bibliographie

- BROWN, O. L. I. et LATIMER, W. M. J. Am. Chem. Soc. 58 : 2228-2229. 1936.
- CASPARI, W. A. J. Chem. Soc. 125 : 2381-2387. 1924.
- DECOPPET, L. C. Ann. chim. phys. (4)25 : 502-553. 1872.
- DECOPPET, L. C. J. Phys. Chem. 8 : 531-538. 1904.
- ENDER, F. Z. Elektrochem. 43 : 234-238. 1937.
- HAMER, W. J. J. Am. Chem. Soc. 56 : 860-864. 1934.
- HARNED, H. S. et EMBREE, N. D. J. Am. Chem. Soc. 56 : 1050-1053. 1934.
- HARNED, H. S. et HAMER, W. J. J. Am. Chem. Soc. 55 : 2194-2206. 1933.
- HILL, A. E. et BACON, L. R. J. Am. Chem. Soc. 49 : 2487-2495. 1927.
- INTERNATIONAL CRITICAL TABLES. McGraw-Hill Book Co., New York. 1927.
- JONES, H. C. Z. physik. Chem. 12 : 623-656. 1894.
- KIELLAND, J. J. Am. Chem. Soc. 59 : 1675-1678. 1937.
- LEWIS, G. N. et RANDALL, M. Thermodynamics and the free energy of chemical substances. McGraw-Hill Book Co., New York. 1923.
- LOOMIS, E. H. Wiedemann's Ann. 57 : 495-520. 1896.
- LOOMIS, E. H. Phys. Rev. 3 : 270-292. 1896.
- MACINNES, D. A. et BELCHER, D. J. Am. Chem. Soc. 55 : 2630-2646. 1933.
- MACINNES, D. A. et BELCHER, D. J. Am. Chem. Soc. 57 : 1683-1685. 1935.
- MARIGNAC, C. Ann. chim. phys. (5)8 : 410-430. 1876.
- MARIGNAC, C. Arch. sci. phys. nat. 55 : 113. 1876.
- MEYERHOFFER, F. W. In Landolt-Börnstein Physikalisch-Chemische Tabellen, I, p. 658. Julius Springer, Berlin. 1923.
- PERREU, J. Compt. rend. 200 : 1030-1032. 1935.
- REDLICH, O. et ROSENFELD, P. In Landolt-Börnstein Physikalisch-Chemische Tabellen, II, p. 113 et seq. Julius Springer, Berlin. 1931.
- RÜMELIN, G. Z. physik. Chem. 58 : 449-466. 1907.
- SWALLOW, J. C. et ALTY, S. J. Chem. Soc. 3062-3079. 1931.
- WALKER, A. C., BRAY, U. B., et JOHNSTON, J. J. Am. Chem. Soc. 49 : 1235-1256. 1927.

THE PHOSPHORUS AND IODINE CONTENTS OF BRITISH COLUMBIA FISH OILS¹

BY R. D. HEDDLE² AND J. S. BRAWN²

Abstract

The amounts of phosphorus and iodine in various British Columbia fish oils have been determined. It has been found that the concentration of phosphorus in the various fish oils is too low to exert much of an antioxidant effect, that samples of fish oil from different localities differ widely in their iodine content, and that fish oils are a relatively high source of iodine.

Introduction

At the present time no data are available on the phosphorus content and little on the iodine content of various fish oils. Such information was deemed of value as it has been shown that organically combined phosphorus present in animal oils may act as an antioxidant retarding the development of rancidity (4) and the destruction of vitamin A (1). The importance of small amounts of iodine in foodstuffs, especially for the prevention of goitre in animals, is well known. Krockert (2), from his investigations, claims that more beneficial results are obtained by feeding iodine organically combined.

Material and Methods

The oils were representative samples of those obtained from fish inhabiting the waters adjacent to British Columbia, and were supplied by Dr. William Chalmers of the Western Chemical Industries, Vancouver. Extensive

TABLE I
RESULTS OF ANALYSES

Oil	Parts of P per million of oil	Parts of lecithin per million of oil	Parts of iodine per million of oil
Dogfish oil	3.2	88.5	3400
Dogfish liver oil	Trace	Trace	3600
Herring oil	8.6	240	2300
Pilchard oil	11.2	310	2300
*"Pilchardine"	9.0	251	2900
Ratfish liver oil	Trace	Trace	3900
**Salmon oil, No. 1	6.2	173	4400
Salmon oil, No. 2	—	—	3200
Salmon oil, No. 3	—	—	2100
Cod liver oil (Norwegian)	7.0	195	4800

* "Pilchardine" is a commercial blend of salmon, pilchard, and greyfish oils.

** Salmon oils obtained from different localities on the Pacific Coast.

¹ Manuscript received in original form June 3, 1940, and, as revised, August 20, 1940.
Contribution from the Department of Chemistry, The University of British Columbia,
Vancouver, B.C.

² Undergraduate student.

preliminary measurements were made using various methods suggested in the literature for the determination both of phosphorus in blood and urine and of iodine in organic substances.

In the case of phosphorus the method finally adopted was a modification of the procedure for the determination of total phosphorus in egg, as described in "Methods of Analyses of Official Agricultural Chemists". The method developed by Mathews, Curtis, and Brode (3), with modifications, was used for the determination of the small amounts of iodine found in the oils.

References

1. HOLMES, H. N., CORBETT, R. E., and HARTZLER, E. R. *Ind. Eng. Chem.*, 28 : 133-135. 1936.
2. KROCKERT, G. *Biedermanns Zentr. B. Tierernahr.*, 7 : 141-157. 1935.
3. MATHEWS, L. N., CURTIS, G. M., and BRODE, W. R. *Ind. Eng. Chem., Anal. Ed.*, 10 : 612-615. 1938.
4. OLCOTT, H. S. and MATTILL, H. A. *Oil & Soap*, 13 : 98-100. 1936.

THE SEPARATION AND IDENTIFICATION OF THE COMPOUNDS PRESENT IN A TURNER VALLEY CRUDE OIL¹

BY L. M. WATSON² AND J. W. T. SPINKS³

Abstract

A large number of compounds present in a Turner Valley crude oil have been separated by fractional distillation in a 3-ft. Stedman column. The fractionation was continued up to 153° C. The compounds have been identified by their physical properties, and the amount of each has been estimated. A comparison with another Turner Valley crude is made.

Introduction

This research deals with the separation, by fractional distillation, of the compounds present in a Turner Valley crude oil and their identification by means of their physical properties. The oil studied is from the Foundation Well No. 1, located in the southern part of Turner Valley. This well was completed in December, 1936, and has a depth of 6474 ft., the producing layer being of Madison limestone. Production from this well totalled about 250,000 barrels to the end of 1939.

Thus far, apart from the work reported by Donald (4), very little has been published concerning the composition of Turner Valley crude oils. Donald has identified most of the compounds boiling between 20° and 80° C. and some of those up to 174° C., and estimated the amount of each in a crude oil from Royalite Oil Company No. 3 Sterling Pacific Well. The present work was undertaken with the idea of confirming his work in so far as the oils are similar and to compare the two oils in regard to constituents and relative amounts over the range of temperature studied.

Experimental Work

Apparatus and Procedure

A 10-gallon sample of the oil was obtained from the Anglo-Canadian Oil Company of Calgary. The crude oil was not lye-washed, as the odour was not objectionable. A preliminary Hempel distillation was carried out to determine the amounts of the various fractions.

Measured at 20° C., 14,000 cc. of the crude oil was fractionated in a Stedman packed column (1) which was 3 ft. long and 1 in. in diameter. In order to avoid possible decomposition, the temperature of the oil in the still was not allowed to exceed 225° C.

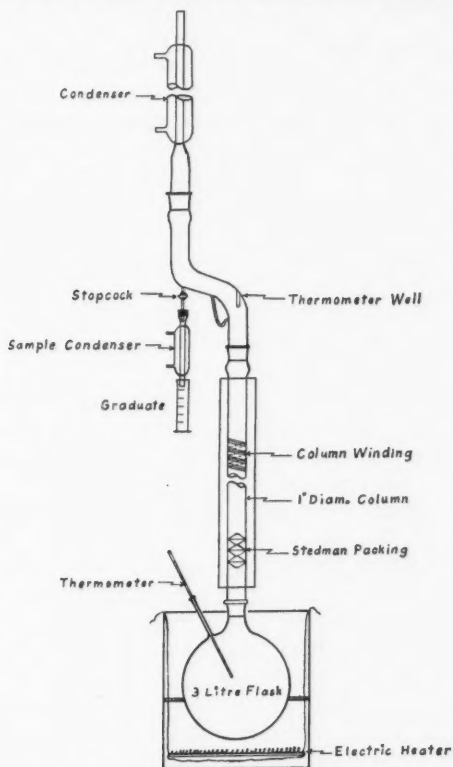
The apparatus is illustrated in Fig. 1. The heater was made by winding 40 ft. of No. 20 Chromel A resistance wire on an octagonal piece of transite

¹ Manuscript received July 2, 1940.

Contribution from the Department of Chemistry, University of Saskatchewan, Saskatoon, Sask., from part of a thesis by L. M. Watson in partial fulfilment of the requirements for the degree of Master of Science.

² Holder of a bursary under the National Research Council of Canada, 1939-1940.

³ Professor of Chemistry.

FIG. 1. *Assembly of fractionating still.*

board. The still pot was placed in an asbestos covered box. The column and still head were insulated with a packing of rock wool 2 in. thick, held in place by a hard paper wrapping. The still head was made of glass and had a stopcock so that the rate of sampling can be adjusted to a suitable value. The column was heated by means of 13 ft. of No. 20 Chromel A wire (0.639 ohm per ft.) wound on it and insulated from the glass with strips of asbestos paper. This column was calibrated from 25° to 200° C. by insulating the ends and applying different currents to the windings. This calibration was necessary for proper temperature control during operation of the column.

The oil was first subjected to a rough fractionation. The reflux ratio in this rough fractionation was estimated to be about 10 to 1. Seven fractions of distillate were obtained over 25° ranges from the initial boiling point to 200° C. These fractions constituted about 60% of the initial charge.

In obtaining a closer fractionation, the first fraction obtained was again charged to the same still. The succeeding fractions were added, as the distillation proceeded, to give an overlapping of about 20° C.

The apparatus was changed slightly for the close fractionation. The thermometer opening that had been used in the rough fractionation was replaced by a thermometer well, and a by-pass tube was added (see Fig. 1) to prevent the cooling of the thermometer by the condensate. The still head was heated by a winding of nichrome wire adjusted so that the temperature of the still head was about 25° C. below that of the column. It was not necessary to use this winding until the temperature of the still head reached 70° C. This heating helps to compensate for the radiation loss from the still head and the thermometer well. A thermometer reading to tenths of a degree was used for determining the temperature of the vapour in the still head for the range from the initial boiling point to 100° C. Above this temperature, a thermometer reading in degrees from 0 to 200° C., and calibrated in the thermometer well, was used.

The column has a maximum efficiency corresponding to about 40 theoretical plates. At the start of the close fractionation, the ratio of reflux to product was about 50 to 1, and this was increased as the temperature increased. The product was collected at a rate of about 6 to 15 cc. per hr. This rate gave the best separation compatible with time available for distillation.

In operating the column, best results are obtained by first flooding it to wet the packing thoroughly. The still was allowed to run three to four hours before sampling to allow attainment of equilibrium in the still head. The column operated satisfactorily at the rates used as shown by the slow rise in the top temperature. Cuts were made at temperatures at which the boiling point was constant for considerable periods, and at other times the cuts were made over a 1° range, providing that a sufficiently large sample was collected for making the required tests. Samples were taken up to 153° C. The temperature of the mid-point of each fraction as obtained from the boiling-point-volume-distilled curve is to be taken as the average boiling point of the fraction. The refractive index for the sodium D line was determined for each sample at 20° C., a Pulfrich Refractometer with temperature control being used. The density of each sample was measured at 20° C. The boiling points were corrected to 760 mm. pressure.

The following plots have been prepared: the boiling point against volume distilled, refractive index against boiling point, and specific refractivity against boiling point.

Experimental Data

Examination of Crude Oil

The general properties of Foundation No. 1 crude oil are as follows:

A. P. I. Gravity at 60° F. = 46.8.

Specific gravity at 60° F. = 0.7936.

Colour—orange.

Viscosity at 100° F. = 33 S.U.

A Hempel distillation on the crude oil gave the results shown in Table I. The volume per cent distilled is plotted against the boiling point in Fig. 2.

The refractive index and density of all the fractions were measured. The aniline points of Fractions 2 to 8 inclusive were determined. The results appear in Table I. The boiling points were estimated from Fig. 2.

The crude oil would be classed as an intermediate base crude on the United States Bureau of Mines Classification.

TABLE I

HEMPEL DISTILLATION OF FOUNDATION WELL CRUDE OIL

Volume of charge = 300 cc. at 60° F. Atmospheric pressure = 720 mm. of mercury.
Room temperature = 23.3° C. Initial boiling point = 25.5° C.

Temperature range, °C.	Volume, % distilled	Sample No.	Density, d_{4}^{20}	Refractive index, n_D^{20}	Aniline point, °C.	Average boiling point, °C.
I.B.P. to 50	8.8	1	0.6316	1.36647		38
50 - 75	6.6	2	.6755	1.38605	56.7	62
75 - 100	8.7	3	.7203	1.40554	49.2	88
100 - 125	10.8	4	.7490	1.41927	44.7	112
125 - 150	8.3	5	.7684	1.43094	44.3	138
150 - 175	7.9	6	.7822	1.43806	48.0	161
175 - 200	6.5	7	.7932	1.44316	55.6	188
200 - 225	6.1	8	.8060	1.44877	61.8	211
225 - 250	6.1	9	.8217	1.45787		236
250 - 275	5.9	10	.8355	1.46513		261
Remainder	22.7					
Loss	1.6					

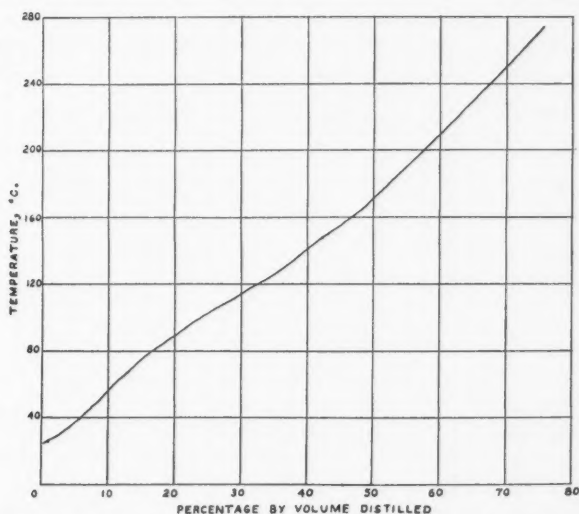


FIG. 2. Hempel distillation. Crude oil—Foundation No. 1. Charge, 300 cc. Atmospheric distillation (720 mm. of mercury). Residue, 22.7%. Loss, 1.6%. Room temperature, 23.3° C.

Fractions 3 to 8 inclusive were treated with twice their volume of concentrated sulphuric acid for 15 min. at 30° C. The acid was separated from the oil, and the oil was subjected to two more acid treatments. The oil was then washed with water, a 10% solution of sodium hydroxide, and then dried over anhydrous calcium chloride. The refractive index, density, and aniline point of the treated fractions were determined. The aniline used was freshly distilled and dried. Data in regard to the treated fractions are given in Table II.

TABLE II
DATA ON THE ACID TREATED FRACTIONS

Sample No.	d_4^{20}	n_D^{20}	Aniline point
3	0.7110	1.39804	58.8
4	.7271	1.40594	61.7
5	.7435	1.41520	64.7
6	.7574	1.42285	68.7
7	.7742	1.43054	71.0
8	.7875	1.43725	74.0

The percentages of paraffins, naphthenes, and aromatics in each fraction were estimated by the graphical method of Kurtz and Headington (6). Table III gives the results in volume per cent.

TABLE III
ESTIMATED COMPOSITION OF HEMPEL SAMPLES

Sample No.	Kurtz and Headington method			Tizard and Marshall method		
	Paraffins	Naphthenes	Aromatics	Paraffins	Naphthenes	Aromatics
1	100					
2	85.6	14.4		78	22	
3	65.0	28.6	6.4	51.3	37.6	11.1
4	46.8	43.3	9.9	48.6	32.3	19.1
5	53.4	29.3	17.3	50.5	27.2	22.3
6	41.2	38.8	20.0	55.8	21.7	22.5
7	38.2	43.3	18.5	46.1	36.7	17.2
8	29.6	52.8	17.6	45.6	40.5	13.9

The aromatics were estimated from the change in aniline point when the aromatics were removed with sulphuric acid, the curves of Tizard and Marshall (8) being used.

The percentages of naphthenes and paraffin in the "residual fraction" were estimated from the aniline point and the average boiling point. These results also appear in Table III.

Since the graphical method has been tested up to 200° C. only, the compositions of the first eight fractions only were estimated. It is seen that the results from the two methods give very poor agreement

These eight fractions constitute 63.7% of the crude oil. From the results of the Kurtz and Headington analyses this part of the oil contains 11.2% aromatics, 57.5% paraffins, and 31.3% naphthenes.

Final Fractionation

The refractive index and density of all the fractions collected were measured and the specific refractivity was calculated. To determine the composition of the fractions, the physical properties measured were plotted as follows: Fig. 3 shows the refractive index plotted against the boiling point; Fig. 4 shows the specific refractivity plotted against the boiling point. The points marked *P*, *N*, and *A* on these graphs represent the values for probable compounds present as given in Tables A, B, and C in the appendix. Fig. 5 shows the volume distilled plotted against the boiling point. Conclusions as to composition are based on the results of the work of the National Bureau of Standards, (cf (7)), physical properties of the fractions, physical properties of known hydrocarbons, and a survey of previous work.

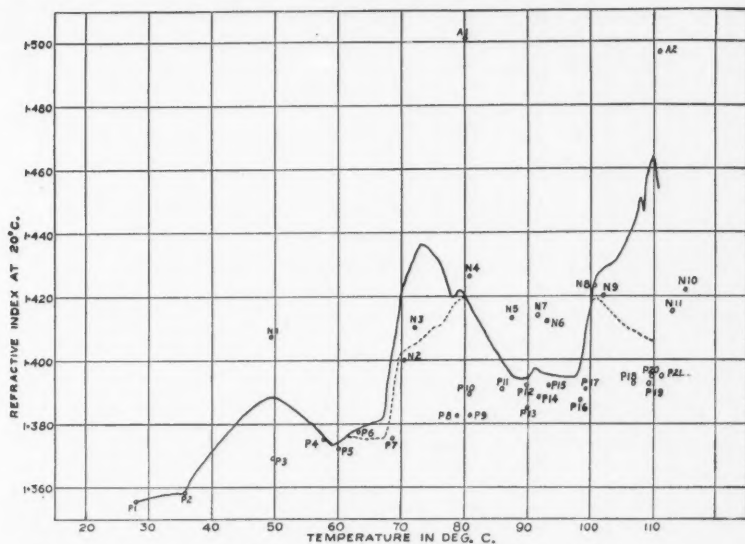


FIG. 3-A. Refractive index vs. boiling point, 20° to 115° C.

Composition of the Fractions

The lighter hydrocarbons were not condensed in the apparatus and so were not determined. By condensing them with an ice mixture, the amount was estimated to be about 1½% by volume, mainly butane. There were probably losses of these due to handling and in transit since, upon opening the samples of the crude oil, a considerable amount of gas escaped.

The first compound to be condensed was isopentane (P1) at 28° C. This was shown by the boiling point curve, and the refractive index and density

measurements checked with these properties as listed for the pure hydrocarbons. *n*-Pentane (P2) was also shown to be present by the break in the boiling point curve and by measurement of its properties.

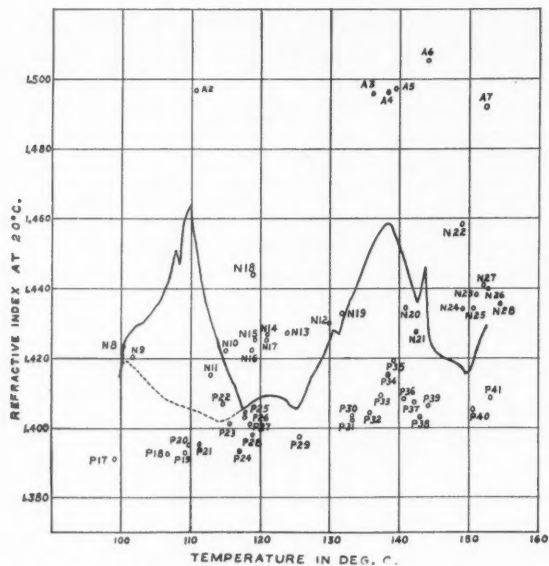


FIG. 3-B. Refractive index vs. boiling point, 115° to 153° C.

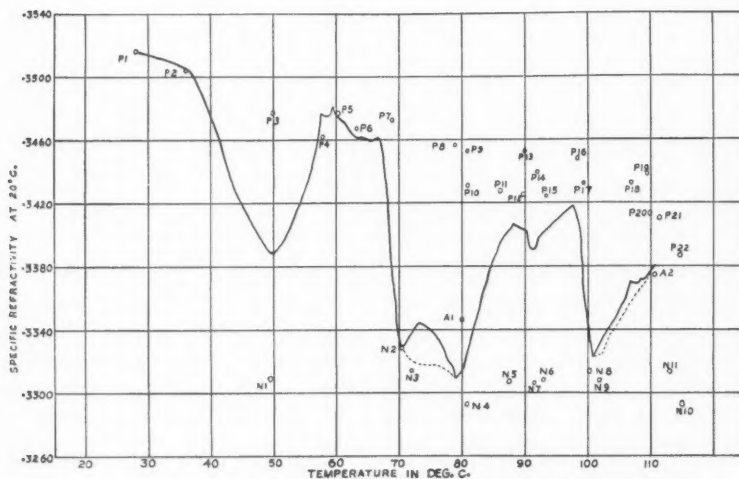


FIG. 4-A. Specific refractivity vs. boiling point, 20° to 115° C.

There is no definite break in the boiling point curve to indicate the presence of cyclopentane (N1), but Fig. 3 and 4 definitely establish its presence. It is seen that 2, 2-dimethylbutane (P3) boils at about the same temperature as the cyclopentane, and so a mixture of the two distills off. By joining the points representing pure cyclopentane, 2,2-dimethylbutane, and *n*-pentane,

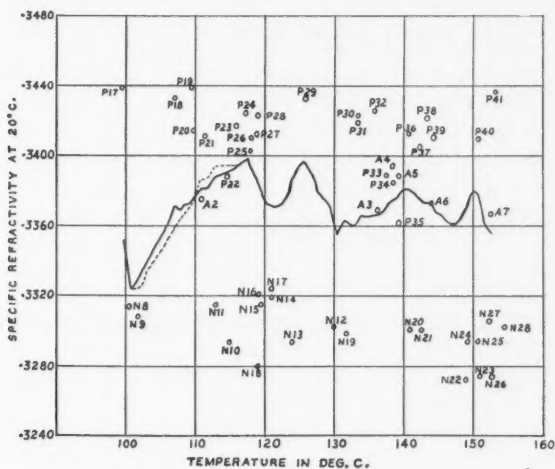


FIG. 4-B. Specific refractivity vs. boiling point, 115° to 153° C.

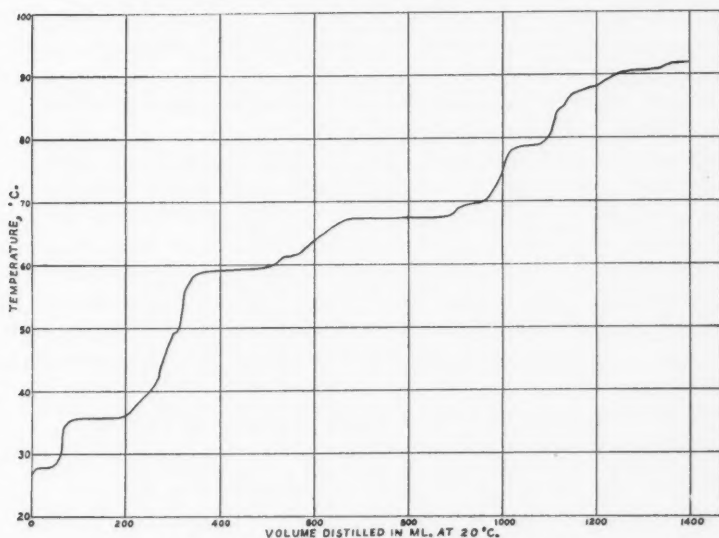


FIG. 5-A. Boiling point vs. volume distilled.

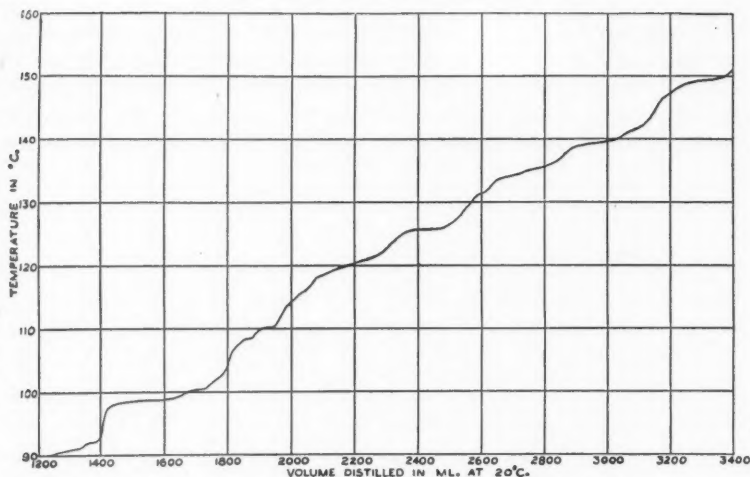


FIG. 5-B. Boiling point vs. volume distilled.

it is possible to calculate the amount of each present in each sample by the position in the triangle. As Donald (4) points out, it is necessary to assume the point where one compound ceases to distil over and another starts to distil off. By choosing the point carefully, the errors tend to balance out. The three compounds may be assumed to distil off together from 36 to 50° C. It is assumed that after this temperature, cyclopentane, 2,2-dimethylbutane, and 2,3-dimethylbutane (P4) distil off together. Donald (4) also estimated the proportion of each by plotting specific refractivity against refractive index and drawing similar triangles.

2,3-Dimethylbutane is indicated by the refractive index curve and by a slight break in the boiling point curve.

2-Methylpentane (P5) is present in large quantities, as shown by the boiling point curve. The break in the curve appears at 59.3° C. The physical properties of the pure compound lie close to that represented by the actual curve.

3-Methylpentane (P6) is also shown to be present by the break in the boiling point curve at 61.5° C., but not in as large a quantity as the 2-methylpentane. The refractive index and the specific refractivity lie very close to the curve.

Benzene (A1) starts to come off at 62° C., so that the refractive index and the density do not fall to the values for *n*-hexane (P7). *n*-Hexane is shown to be present in large amounts by the break in the boiling point curve at 67.5° C.

Nitration of all the samples containing benzene was carried out to remove the benzene as *m*-dinitrobenzene, as outlined in Reference (3). The melting points of the dried nitro product were in all cases close to the melting point of *m*-dinitrobenzene (89.7° C.) and could be raised to that point by recrystallization. Benzene was found to be present in all the samples in the boiling

point range from 62 to 80.7° C. The fraction with boiling point of 69.2° C. had the highest concentration of benzene, 7.8% by weight. Most of the benzene is present in the fraction boiling between 66 and 70° C. The refractive index and density of the samples containing benzene were determined after removal of the benzene, and the refractivity and refractive index were plotted against the original boiling point of the sample as shown by the dotted lines in Fig. 3 and 4.

There is a break in the boiling point curve at 69.8° C. This is probably a continuation of the *n*-hexane-benzene mixture. However, there would seem to be the possibility that this was due to ethyl cyclobutane (N2), b.p., 70.5. This compound has not been detected in the work of the National Bureau of Standards on the constitution of petroleum, so that its presence is extremely doubtful, although in Fig. 4 it is seen to fall on the experimental curve. Fig. 3 does not show any break corresponding to methylcyclopentane (N3). In Fig. 4 the curve drops rapidly, showing definitely that it is present. The specific refractivity reaches a minimum at methylcyclopentane, rises, and then falls to a minimum corresponding to cyclohexane (N4). The slight rise in the refractive index curve Fig. 3 is also probably due to cyclohexane since the curve appears to be falling steadily from its maximum at 72° C. The break in the boiling point curve at 69 to 70° is due to a mixture of benzene, *n*-hexane and methylcyclopentane (5). The break at 79° C. is due to a mixture of benzene and cyclohexane (2) with other hydrocarbons, mainly 2,2-dimethylpentane (P8).

The branched heptanes boil in the range 80 to 100° C. and cause the drop in the refractive index curve after the cyclohexane area. These would be inseparable from the dimethylcyclopentanes, which boil from 87.5 to 93° C. It is these naphthenic compounds that cause the rise in the refractive index curve at 91.5° and the minimum in the specific refractivity curve at the same temperature. The break in the boiling point curve at 87.5° is probably due to 1,1-dimethylcyclopentane (N5) and 2-methylhexane (P13). The compound coming off in large quantities at 90.5° is quite likely 2-methylhexane as reported by Bruun and Hicks-Bruun. 2,3-Dimethylpentane (P12) was not found by the National Bureau of Standards and is probably not present in this case. The compound present at 92° C., as shown by the boiling point curve, is probably 3-methylhexane (P14).

The break in the boiling point curve at 98.5° C. is undoubtedly due to *n*-heptane (P16), which is present in large amounts. Its presence is also shown by the refractive index curve and by the peak in the specific refractivity curve at 98° C.

The presence of a naphthene at 100.5° C. is indicated by the boiling point curve and refractive index, and also by the minimum in the specific refractivity curve. The naphthene is probably methylcyclohexane (N8), as reported by the National Bureau of Standards, but since ethylcyclopentane (N9) has almost the same properties, some of the latter may be present.

Toluene (A2) starts to distil at 92° C. It was removed from the samples by nitration according to the method used by the National Bureau of Standards (3). The melting points of the dried nitro product were close to that of pure dinitrotoluene (70° C.) and could be raised to that point by recrystallization. The percentage by weight of toluene in the fraction increases from 0.02 at 92° C. to 4.8 at 100.3° C. After this point the percentage of toluene in the samples increases rapidly, reaching a maximum of about 60% at 110° C., the boiling point of toluene. The refractive index and density of the samples were determined after the removal of the toluene, and the specific refractivity and refractive index were plotted against the original boiling point of the sample, as shown by the dotted lines in Figs. 3 and 4.

The breaks in the boiling point curve at 108.5° and at 110° C. are probably due to mixture of toluene and the dimethylhexanes. The first break is confirmed by the dip in the refractive index curve at 108.5° C.

Not many octanes are present, as shown by the rapid rise of the boiling point from 110 to 118° C. There is a break in the boiling point curve at 118° C., probably due to 4-methylheptane (P26), 3-methylheptane (P28), and 2-methylheptane (P24). Their presence is also shown by the minimum in the refractive index curve at this temperature.

The flat slope of the boiling point curve between 119 and 123° C. is due to the dimethylcyclohexanes (N12-N17). Their presence is corroborated by the peak in the refractive index curve at 121° C. and by the minimum in the specific refractivity curve at 121.5° C. The National Bureau of Standards has found 1,3-dimethylcyclohexane (N14), 1,2-dimethylcyclohexane (N13) and an octanaphthene (119.8° C.) to be present. They report cycloheptane (N18) as probably being absent.

n-Octane (P29) is shown to be present by the break in the boiling point curve, the minimum in the refractive index curve, and the peak in the specific refractivity, all at 125.5° C.

The minimum in the specific refractivity curve at 130.5° C. indicates the presence of ethylcyclohexane (N19). This compound probably causes the slight break in the boiling point curve at 131.8° C.

The refractive index curve indicates the presence of aromatics in the fractions in the boiling range 130 to 140° C. These could be estimated by removing them by nitration. The curves indicate that the aromatics are the three xylenes (A4, A5, and A6) and ethylbenzene (A3), all of which have been isolated from crude petroleum. The breaks in the boiling point curve at 134, 139, and 141° C. are due to mixtures of these aromatics with paraffins.

The specific refractivity curve indicates the presence of a naphthene at 147° C. This is in agreement with Donald's results, and a nonanaphthene has been reported at this temperature by Tongberg, Fenske, and Sweeney (9).

n-Nonane (P40) is shown to be present by the peak in the specific refractivity curve at 150.5° C., the minimum in the refractive index curve at 150° C., and the break in the boiling point curve at 149.5° C.

The rapid rise in the refractive index curve after 150° C. indicates the presence of an aromatic, probably isopropylbenzene, while the rapid fall in the specific refractivity curve after 150° C. indicates the presence of a naphthene.

Lack of time prevented the final fractionation from being carried on beyond this point. However, at these higher temperatures, the number of possible compounds present is very great and it is difficult to draw conclusions as to which may be present, and almost impossible to estimate the amounts of those known to be present.

Estimation of Compounds Present in the Crude

It has been stated before, for the case of cyclopentane, 2,2-dimethylbutane, and *n*-pentane, that it is possible to calculate the amount of a certain compound present in a sample from the physical properties of the sample. However, it is necessary to assume the point where one compound ceases to distil over and another starts to distil. With rising temperature there is increased difficulty in knowing which compounds are present, and therefore there is greater error in the estimation of the amounts of the compounds. The estimates of the percentages of the compounds present in the petroleum up to 80° C., however, are fairly reliable since the compounds in this range are not so numerous.

By plotting specific refractivity against refractive index for cyclohexane, benzene, and methylcyclohexane, the amounts of these compounds present in the samples were estimated by the position of the samples in the triangle formed by these three compounds. This was the method used by Donald (4). Similar triangles were drawn in the estimation of other compounds.

Table IV is a list of the compounds detected boiling in the range from 25 to 81° C. with the estimated percentage by volume of each in the crude oil. The values obtained by Donald for No. 3 Sterling Pacific Well are shown for comparison.

TABLE IV
COMPOUNDS BOILING BELOW 81° C.

Compound	Boiling point, °C. at 760 mm.	Estimated % in crude	Estimated % in Sterling Pacific No. 3
Isopentane	28.0	0.36	0.38
<i>n</i> -Pentane	36.0	0.90	0.79
Cyclopentane	49.5	0.14	0.09
2,2-Dimethylbutane	49.7	0.14	0.11
2,3-Dimethylbutane	58.1	0.25	0.27
2-Methylpentane	60.2	0.80	0.94
3-Methylpentane	63.2	0.44	0.56
<i>n</i> -Hexane	68.7	1.30	2.40
Methylcyclopentane	72.1	0.55	0.82
Benzene	80.2	0.28	0.32
Cyclohexane	80.8	0.41	0.76

The estimation of the amounts of the compounds present in the boiling range from 80 to 153° C. is a rough approximation and gives only the order of magnitude. This is due to the difficulty of knowing which compounds are present, the large number of compounds present, and also the difficulty of obtaining close fractionation. The amounts of toluene, *n*-heptane, and methylcyclohexane were determined in a manner similar to that used for benzene, *n*-hexane, and methylcyclopentane. The estimations are more reliable for those compounds present in large amounts.

Table V gives an estimate of the compounds detected in the 80 to 153° C. range. The values given by Donald for No. 3 Sterling Pacific Well are shown for comparison.

TABLE V
COMPOUNDS BOILING BETWEEN 80° AND 153° C.

Compound	Estimate % by volume in crude	Sterling Pacific No. 3
Dimethylcyclopentane	0.71	0.75
2-Methylhexane	0.90	1.0
3-Methylhexane	0.60	0.7
<i>n</i> -Heptane	1.40	1.6
Methylcyclohexane	0.90	2.2
Ethylcyclopentane		
Toluene	1.07	2.0
2-, 3-, and 4-Methylheptane	0.55	0.5
Dimethylcyclohexanes	0.50	0.8
<i>n</i> -Octane	1.00	0.95
Ethylcyclohexane	0.65	0.6
Threexylenes	1.45	2.5
Ethylbenzene		
<i>n</i> -Nonane	0.80	0.8

Discussion

The compounds detected in this work agree with those reported by Donald. The refractive index and specific refractivity curves for both crudes show maxima and minima at virtually the same temperatures. This research confirms Donald's results and indicates that the compounds present in these two Turner Valley crude oils are virtually the same.

The estimated percentages of the compounds present as given in Table IV agree in magnitude with those given by Donald. The greatest difference lies in the amount of *n*-hexane estimated. Fair agreement between the amounts of the compounds present is also noted in Table V. The percentages of benzene and toluene reported are quite reliable since they were determined by nitration. No strict comparison of the estimated amounts of the other compounds can be made as these amounts are only approximate.

It is seen that the distillation curve for the final fractionation (Fig. 5) is characterized by horizontal portions separated by transition sections. These horizontal portions are usually of simple composition, and the changes

of slope in the curve give the points of cut for the various fractions. A study of these fractions would be of great value in refinery operation. Such a study would show the possibility of combining various narrow boiling point fractions to produce a fuel of high octane rating which at the same time has the other essential properties of a good gasoline.

This study indicates once more the value of Stedman columns in determining the true boiling point curve of petroleum. Analysis of the fractions would indicate the compounds present and their amount, thus showing the feasibility of the separation of these compounds in virtually pure state by fractionation.

The work is being extended to cover other western Canadian crude oils.

Acknowledgments

The authors are indebted to the National Research Laboratories, Ottawa, for the loan of a Stedman column. The Anglo-Canadian Oil Company of Calgary kindly donated the sample of crude oil. The helpful suggestions given by Dr. T. Thorvaldson of the University of Saskatchewan and Mr. R. M. Donald of Moose Jaw have been greatly appreciated.

References

1. BRAGG, L. B. Refiner, 18 : 295-298. 1939.
2. BRUUN, J. H. and HICKS-BRUUN, M. M. Bur. Standards J. Research, 7 : 607-615. 1931.
3. BRUUN, J. H. and HICKS-BRUUN, M. M. Bur. Standards J. Research, 6 : 869-880. 1931.
4. DONALD, R. M. National Research Council Report: "The Fractionation of Turner Valley Crude Oils using Stedman Columns"; Can. J. Research, B, 18 : 12-29. 1940.
5. BRUUN, J. H. and HICKS-BRUUN, M. M. Bur. Standards J. Research, 7 : 799-809. 1931.
6. KURTZ, S. S. and HEADINGTON, C. E. Ind. Eng. Chem. Anal. Ed. 9 : 21-25. 1937.
7. ROSSINI, F. D. Refiner, 16 : 545-562. 1937.
8. TIZARD and MARSHALL, A. G. J. Soc. Chem. Ind. 40 : 20-25T. 1921.
9. TONGBERG, C. O., FENSKE, M. R., and SWEENEY, W. J. Ind. Eng. Chem., 30 : 166-169. 1938.

An appendix follows, on pages 402-404.

APPENDIX
Properties of Hydrocarbons

TABLE A
PARAFFINIC COMPOUNDS

No.	Compound	B.p., °C.	d_4^{20}	n_D^{20}	S.R.*
P 1	Isopentane	27.95	0.62007	1.355	0.35146
P 2	<i>n</i> -Pentane	36.0	.62632	1.35769	.3503
P 3	2,2-Dimethylbutane	49.8	.6493	1.3692	.34768
P 4	2,3-Dimethylbutane	57.92	.6612	1.3750	.3462
P 5	2-Methylpentane	60.24	.6532	1.3718	.3477
P 6	3-Methylpentane	63.16	.6642	1.3775	.3467
P 7	<i>n</i> -Hexane	68.76	.6595	1.3752	.34726
P 8	2,2-Dimethylpentane	78.9	.6737	1.38233	.34569
P 9	2,4-Dimethylpentane	80.8	.6745	1.38233	.34528
P10	2,2,3-Trimethylbutane	80.9	.6900	1.38940	.34308
P11	3,3-Dimethylpentane	86.0	.6934	1.39114	.34277
P12	2,3-Dimethylpentane	89.7	.6952	1.39201	.34263
P13	2-Methylhexane	90.0	.6789	1.38509	.34527
P14	3-Methylhexane	91.8	.6870	1.38873	.34404
P15	3-Ethylpentane	93.3	.6952	1.39201	.34254
P16	<i>n</i> -Heptane	98.4	.6836	1.38777	.34493
P17	2,2,4-Trimethylpentane	99.3	.6918	1.3916	.34389
P18	2,2-Dimethylhexane	106.9	.6953	1.3930	.34327
P19	2,5-Dimethylhexane	109.4	.69378	1.39297	.34385
P20	2,4-Dimethylhexane	109.8	.7030	1.3955	.3414
P21	3,3-Dimethylhexane	111.3	.710	1.3955	.34109
P22	2,3,3-Trimethylpentane	114.6	.7253	1.4072	.33878
P23	2,3-Dimethylhexane	115.8	.7118	1.4015	.34174
P24	2-Methylheptane	117.2	.6980	1.3936	.34238
P25	3,4-Dimethylhexane	117.9	.7193	1.4044	.34029
P26	4-Methylheptane	118.0	.7165	1.4035	.34098
P27	3-Ethylhexane	118.6	.7128	1.4014	.34115
P28	3-Methylheptane	119.0	.7054	1.3982	.34230
P29	<i>n</i> -Octane	125.68	.70256	1.39758	.34326
P30	2,4-Dimethylheptane	133.3	.7167	1.4036	.34226
P31	2,6-Dimethylheptane	133.2	.7129	1.4025	.34194
P32	2,5-Dimethylheptane	135.8	.7142	1.4042	.34258
P33	3,3-Dimethylheptane	137.5	.7304	1.4095	.33885
P34	4-Ethylheptane	138.5	.7407	1.41564	.33854
P35	3,3-Diethylpentane	139.2	.75222	1.4197	.33623
P36	2,3-Diethylpentane	140.6	.7235	1.4085	.34128
P37	4-Methyloctane	142.2	.7243	1.4078	.34045
P38	2-Methyloctane	143.2	.7134	1.4032	.34220
P39	3-Methyloctane	144.2	.7210	1.4065	.34105
P40	<i>n</i> -Nonane	150.72	.71780	1.40541	.34096
P41	2,4-Dimethyloctane	153.1	.7244	1.4090	.34368
P42	2,6-Dimethyloctane	159.0	.7288	1.4114	.34097
P43	3,6-Dimethyloctane	160.0	.7364	1.4145	.33969
P44	5,7-Dimethyloctane	160.25	.7254	1.4084	.34035
P45	4- <i>n</i> -Propylheptane	161.7	.7360	1.414	.33953
P46	5-Methylnonane	165.1	.73255	1.4122	.34308
P47	4-Methylnonane	165.7	.73234	1.4123	.33996
P48	2-Methylnonane	166.8	.72805	1.4099	.34022
P49	3-Methylnonane	167.8	.73335	1.4125	.33965
P50	<i>n</i> -Decane	174.02	.73014	1.41191	.34071

* B.p.—Boiling point at 760 mm. d_4^{20} —Density at 20° C. n_D^{20} —Refractive index at 20° C. with sodium D line. S.R.—Lorentz-Lorenz specific refractivity.

TABLE B
NAPHTHENIC COMPOUNDS

No.	Compound	B.p., °C.	d_4^{20}	n_D^{20}	S.R.
N 1	Cyclopentane	49.5	0.7447	1.4075	0.3309
N 2	Ethylcyclobutane	70.5	.7284	1.4004	.33293
N 3	Methylcyclopentane	72.1	.7482	1.4103	.33137
N 4	Cyclohexane	80.8	.7785	1.4263	.32933
N 5	1,1-Dimethylcyclopentane	87.5	.7552	1.4139	.33082
N 6	1,2-Dimethylcyclopentane	93.0	.7534	1.4126	.3309
N 7	1,3-Dimethylcyclopentane	91.5	.7563	1.4144	.33069
N 8	Methylcyclohexane	100.4	.7695	1.4237	.33143
N 9	Ethylcyclopentane	101.8	.7654	1.4202	.33077
N10	1,1,3-Trimethylcyclopentane	115.0	.7703	1.4223	.32926
N11	1,2,4-Trimethylcyclopentane	113.0	.7565	1.4156	.33144
N12	1,2-Dimethylcyclohexane (cis)	130.0	.7822	1.4303	.33025
N13	1,2-Dimethylcyclohexane (trans)	124.0	.7799	1.4273	.32944
N14	1,3-Dimethylcyclohexane (cis)	121.0	.7735	1.4269	.33185
N15	1,3-Dimethylcyclohexane (trans)	119.4	.772	1.4254	.33146
N16	1,4-Dimethylcyclohexane (cis)	119.0	.7638	1.4223	.33206
N17	1,4-Dimethylcyclohexane (trans)	121.0	.7727	1.4253	.33244
N18	Cycloheptane	118 - 120	.8099	1.4440	.3280
N19	Ethylcyclohexane	131.8	.78804	1.43304	.32984
N20	1,2,3-Trimethylcyclohexane	141.0	.7898	1.4346	.3301
N21	1-Methyl-2-isopropylcyclopentane	142.5	.7792	1.4279	.3301
N22	Cyclooctane	149.0	.8349	1.4586	.3272
N23	1,1-Diethylcyclopentane	151.0	.8028	1.4388	.3275
N24	1,3-Diethylcyclopentane	149.2	.791	1.4343	.32940
N25	1,4-Diethylcyclopentane	150.6	.791	1.4343	.3294
N26	1,2-Diethylcyclopentane	152.6	.805	1.4400	.3274
N27	Isopropylcyclohexane	152.3	.799	1.4411	.33063
N28	Propylcyclopentane	154.5	.793	1.4369	.33033
N29	1,2,3,4-Tetramethylcyclohexane	161.0	.7934	1.4371	.3303
N30	1-Methyl-3-isopropylcyclohexane	168.5	.7948	1.4380	.32922
N31	1-Methyl-4-isopropylcyclohexane	170.0	.7974	1.4380	.32844
N32	1-Methyl-2-isopropylcyclohexane	171.0	.8135	1.4147	.33102
N33	Isoamylcyclopentane	171.5	.7868	1.4340	.33105
N34	Isobutylcyclohexane	171.5	.797	1.4391	.33008

TABLE C
AROMATIC COMPOUNDS

No.	Compound	B.p., °C.	d_4^{20}	n_D^{20}	S.R.
A 1	Benzene	80.112	.87896	1.50123	.33475
A 2	Toluene	110.68	.8669	1.49685	.33747
A 3	Ethylbenzene	136.15	.8669	1.49587	.3369
A 4	<i>p</i> -Xylene	138.40	.8610	1.49613	.33937
A 5	<i>m</i> -Xylene	139.30	.8641	1.49741	.33887
A 6	<i>o</i> -Xylene	144.05	.88011	1.50547	.33729
A 7	Iso-Propylbenzene	152.53	.8620	1.4922	.33668
A 8	<i>n</i> -Propylbenzene	159.45	.86214	1.4922	.33665

TABLE C—*Concluded*
AROMATIC COMPOUNDS—*Concluded*

No.	Compound	B.p., °C.	d_4^{20}	n_D^{20}	S.R.
A 9	1-Methyl-3-Ethylbenzene	160.0	.8690	1.4975	.33812
A10	1-Methyl-4-Ethylbenzene	162.4	.8619	1.4946	.33702
A11	1-Methyl-2-Ethylbenzene	164.9	.8826	1.5048	.33594
A12	1,3,5-Trimethylbenzene	164.65	.8654	1.4992	.33945
A13	1,2,4-Trimethylbenzene	169.18	.8762	1.5048	.33939
A14	<i>tert</i> -Butylbenzene	168.9	.8669	1.4925	.33494
A15	Isobutylbenzene	170.5	.8668	1.4934	.33506
A16	<i>sec</i> -Butylbenzene	173.50	.8623	1.4901	.3348
A17	1,2,3-Trimethylbenzene	176.10	.8951	1.5139	.3363

A PROPOSED MODIFICATION OF EMMERIE'S IRON-DIPYRIDYL METHOD FOR DETERMINING THE TOCOPHEROL CONTENT OF OILS¹

BY W. E. PARKER² AND W. D. MCFARLANE³

Abstract

By treating a petrol ether solution of wheat-germ oil with 85% sulphuric acid, centrifuging, and washing the supernatant petrol ether with dilute alkali, carotenoids and other substances that interfere with the iron-dipyridyl method for determining tocopherol are removed. Tocopherol is not affected by the treatment. The tocopherol content of the solution is finally determined by a modification of Emmerie's method.

Introduction

The iron-dipyridyl method of determining tocopherols introduced by Emmerie (2) is much more sensitive than the more specific nitric acid method of Furter and Meyer (3) and is more generally applicable than the spectrographic methods used by Drummond (1) and Moore (5), or the potentiometric titration employed by Karrer (4). However, as Emmerie has pointed out, many substances present in oils may interfere with the test, either by reducing ferric iron or by obscuring the colour of ferrous dipyridyl. He therefore recommends that oils be saponified, and that the carotenoid pigments be removed from the unsaponifiable fraction by adsorption on Floridin XS earth before the test is carried out.

The writers' attempts to apply the method to wheat-germ oil were unsuccessful. Determinations carried out on an unsaponified oil dissolved in hexane gave apparent tocopherol values ranging from 175 to 550 mg. per 100 gm. of oil; the more dilute the oil solution, the higher was its apparent tocopherol content. The colour did not reach a maximum on standing in the dark, but slowly increased in intensity for several hours. These results confirmed Emmerie's statement that the unsaponifiable fraction of the oil should always be used for tocopherol determinations. The writers were anxious, however, to work with unsaponified oils if possible, because of the known instability of tocopherols in alkaline solution, and sought other means of eliminating interfering substances from the oil.

Experimental

The writers have found that the iron-dipyridyl method gives excellent results when applied to solutions of synthetic *d,l*, α -tocopherol. Measurements with an Evelyn photoelectric colorimeter showed that over the range of concentrations studied (16.8 to 168 micrograms of tocopherol per ml.) the

¹ Manuscript received July 24, 1940.

Contribution from the Faculty of Agriculture of McGill University, Macdonald College, Que. Macdonald College Journal Series No. 143.

² Senior Demonstrator, Department of Chemistry, Macdonald College.

³ Professor of Chemistry, Macdonald College.

intensity of the red colour obeyed Beer's law. The value of K was found to be 0.0564 ± 0.0001 , with a maximum deviation of 0.0010. The maximum intensity of colour was reached almost immediately on adding the reagents, and no appreciable increase relative to the blank was noted after the solution had stood in the dark for 15 min.

One possibility of separating some of the interfering pigments from tocopherol was suggested by the well known instability of the carotenoids in acid solution. Tocopherols, on the other hand, are known to be relatively stable in the presence of acid. Test tube experiments showed that concentrated sulphuric acid added to a hexane or petrol ether solution of wheat-germ oil resulted in the separation of all the pigments as a brown mass in the acid, leaving a water-clear supernatant phase, which reduced ferric iron in the presence of dipyridyl.

More extensive tests of the effect of strong sulphuric acid on carotenoid pigments, tocopherol, and oil were then carried out. Sulphuric acid of a concentration of 85% or greater removed carotene and xanthophyll completely from petrol ether solution; the residual petrol ether did not yield any red colour with ferric iron and dipyridyl.

A solution of synthetic α -tocopherol in petrol ether was then tested with sulphuric acid of various strengths by shaking 50 ml. portions with 10 ml. of the acid in a separatory funnel. The tocopherol content of the solution was determined before the addition of acid, and again after the acid phase had been completely separated. It was found that sulphuric acid in concentrations up to 88% apparently had no effect on tocopherol. Acid of 90% concentration or greater removed tocopherol from the petrol ether phase. In the latter case the appearance of a clear yellow colour in the sulphuric acid was also evidence of some reaction between the tocopherol and the more concentrated acid. This yellow colour disappeared when the sulphuric acid was diluted, but apparently the tocopherol did not re-enter the petrol ether phase. Washing with alkali of varying concentrations up to 8% sodium hydroxide did not affect the tocopherol content of the solution. The effect of stronger alkali was not investigated.

The possibility still remained that, although the petrol ether solution reduced ferric iron after treatment with sulphuric acid, the reducing material might be some decomposition product of tocopherol rather than tocopherol itself. Therefore ultra-violet absorption measurements were carried out on a tocopherol solution before and after treatment with 88% sulphuric acid. Since in both cases the solution exhibited maximum absorption at 2940 Å, and the two extinction coefficients were identical, it was concluded that the tocopherol passed through the acid treatment unchanged.

Tests of the effect of 85 to 88% sulphuric acid on petrol ether solutions of wheat-germ and other oils definitely established the following points:

1. All pigments could be removed from the oil solution by the sulphuric acid treatment. Sterols were removed also, as the residual oil from

which the petrol ether had been evaporated failed to give the Liebermann-Burchard test.

2. Treatment with acid did not remove all the reducing substances which interfered with the Emmerie test. Some material that slowly reduced ferric iron was still present.
3. Washing the acid-treated petrol ether solution with dilute alkali (1% potassium hydroxide solution) removed the interfering substance(s). Solutions thus treated reduced ferric iron immediately, as did tocopherol, and on standing in the dark the test solution showed little or no increase in colour intensity relative to the control solution.
4. The unsaponifiable fraction of acid-treated oil exhibited the ultra-violet absorption band at 2940 Å characteristic of α -tocopherol.
5. Synthetic tocopherol added to wheat-germ oil was recovered after acid treatment. Recoveries of 101.5, 96.5, and 99.2% were obtained.
6. Corn oil, arachis oil, linseed oil, and oleic acid, when treated with acid and washed with alkali, did not reduce ferric iron. Olive oil gave a very slight reduction.
7. Solutions of between 1–2% of the oil in petrol ether, normal hexane, or redistilled *varnish maker's* naphtha (b.p. 120 to 140°) were found most suitable for treatment with acid. Within this range of concentrations there is no appreciable rise in temperature on addition of the acid. The naphtha is probably the best solvent since changes in volume during the determination are less likely to take place. Other solvents, such as benzene, cyclohexane, ethyl ether, and chloroform were unsatisfactory.

The following reagents and procedure were finally adopted for carrying out the determination.

Description of the Method

Reagents

1. Petrol ether, normal hexane, or naphtha. The solvent is purified by shaking with concentrated sulphuric acid, washing with 2 *N* alkali, and distillation.
2. Sulphuric acid solution containing 85 parts of concentrated acid (sp. gr. 1.86) and 15 parts of water.
3. Potassium hydroxide. 1% solution.
4. Absolute ethanol or isopropyl alcohol purified as follows:

To 100 ml. of alcohol add about 2 gm. of ferric nitrate. Let stand in the dark for at least 48 hr. Distil in subdued light and store the alcohol in a brown glass bottle.
5. Ferric chloride, 0.1% (approximately) solution of ferric chloride (Merck reagent crystals) in purified absolute ethanol or isopropyl alcohol.
6. α - α' -Dipyridyl, 0.1% (approximately) in purified absolute ethanol or isopropyl alcohol.

Procedure

To 10 ml. of a 1 to 2% petrol ether, hexane, or naphtha solution of the oil in a 15 ml. glass-stoppered centrifuge tube, 2 ml. of the sulphuric acid reagent was slowly added from a pipette. The tube was stoppered and inverted several times until the brown emulsion first formed was broken and settled rapidly. The tube was then centrifuged for two minutes. As much of the clear petrol ether layer as possible was decanted into a second centrifuge tube and 5 ml. of 1% potassium hydroxide solution added. The mixture was shaken, and again centrifuged. An aliquot of the petrol ether phase containing 40 to 100 micrograms of tocopherol was transferred to an Evelyn Colorimeter tube, 1 ml. each of the dipyridyl and ferric chloride reagents added, and then absolute alcohol or isopropyl alcohol to give a total volume of 10 ml. A solution containing 1 ml. of petrol ether, 1 ml. of each of the reagents, and 7 ml. of absolute alcohol or isopropyl alcohol, prepared at the same time as the test solution, was used to adjust the setting of the colorimeter, and served also as a control on any colour due to ferrous iron in the reagents. Measurements of colour intensity were made immediately.

TABLE I

THE TOCOPHEROL CONTENT OF VARIOUS SAMPLES OF WHEAT-GERM OIL, AS DETERMINED BY THE MODIFIED METHOD

Expressed oil	Mg. of Tocopherol per 100 gm. of oil	Solvent extracted oil	Mg. of Tocopherol per 100 gm. of oil
Sample 1	{ 310 308	Sample 1	{ 334 326 326 334 330
Sample 2	{ 323 326	Sample 2	{ 370 375

Several samples of wheat-germ oil have been analyzed for tocopherol by this method. Successive measurements on the same oil agree closely, (Table I). The results are somewhat higher than those reported for methods employing alkaline saponification, but the writers have found that careful hydrolysis of one of the oils with a minimum of absolute alcoholic potash in an atmosphere of nitrogen for 30 min. yielded an unsaponifiable fraction that apparently contained as much tocopherol as the acid treated oil. A large excess of alkali, or long-continued heating, reduced the tocopherol content of the unsaponifiable residue to less than half of its original value.

Acknowledgments

This work was supported in part by a grant from the Ogilvie Flour Mills Co. Limited, Montreal, who also supplied the extracted wheat-germ oil. Merck and Company Limited, Montreal, kindly supplied the writers with synthetic *d,l*, α -tocopherol.

References

1. CUTHBERTSON, W. F. J., RIDGEWAY, R. R., and DRUMMOND, J. C. *Biochem. J.* 34 : 134-139. 1940.
2. EMMERIE, A. and ENGEL, CHR. *Rev. trav. Chim.* 57 : 1351-1355. 1933.
3. FURTER, M. and MEYER, R. E. *Helv. Chim. Acta.* 22 : 240-250. 1939.
4. KARRER, P. and KELLER, H. *Helv. Chim. Acta.* 22 : 617-618. 1939.
5. MOORE, T. and RAJAGOPAL, K. R. *Biochem. J.* 34 : 335-342. 1940.

STUDIES ON HOMOGENEOUS FIRST ORDER GAS REACTIONS

XII. THE DECOMPOSITION OF GLYOXAL TETRA-ACETATE¹BY J. C. ARNELL², J. R. DACEY³, AND C. C. COFFIN⁴

Abstract

The decomposition of gaseous glyoxal tetra-acetate to acetic anhydride and glyoxal is homogeneous and unimolecular. Both the activation energy and the temperature independent factor of the first order rate constant are substantially larger than in the case of the diacetate esters. The decomposition velocity is given by the equation $k = 1.8 \times 10^{12} e^{-39200/RT}$.

Introduction

It is recognized that gas reactions proceeding by the unimolecular mechanism are much more numerous than was formerly supposed, particularly among the complex molecules of organic chemistry. Examples suitable for a study of the effect of structure on molecular stability are, however, very difficult to find. Such reactions must be clean cut, homogeneous and strictly localized within the molecule. They must take place at a convenient rate at temperatures low enough to eliminate the possibility of free radicals and be free from the suspicion of reaction chains. The molecules of the reacting series should be capable of a wide variety of structural alterations.

The decompositions of the methylene diacetate homologues dealt with in earlier papers (for references see (7)) of this series appear to fulfil the above conditions in a satisfactory manner and have led to certain conclusions regarding the effect of molecular structure on the rate of this type of reaction. Thus the activation energy was found to be the same (33,000 cal.) for all these decompositions, which are also alike in having smaller (10^9 to 10^{11}) temperature factors than those usually characteristic of unimolecular reactions. No change in rate was effected by adding $-\text{CH}_2-$ groups to the anhydride chains and only small changes by like additions to the aldehyde end (2). In the latter case the rate increased by small and gradually diminishing increments until the four carbon compound was reached when the effect vanished all together. Thus the butylidene and heptylidene esters, for example, have the same decomposition velocity at all temperatures (2, 5). Practically no change in rate was brought about by substituting three chlorines for three aldehyde hydrogens of the ethylidene ester (9). Concentration was also found to have no measurable effect—the decomposition rate being the same in the pure liquid state as in the gaseous state at 0.1 mm. pressure (7, 8, 9).

¹ Manuscript received September 26, 1940.

Contribution from the Laboratory of Physical Chemistry, Dalhousie University, Halifax, N.S.

² Graduate Student and holder (1939–1940) of a Bursary under the National Research Council of Canada, at Dalhousie University. Present address McGill University, Montreal.

³ Graduate Student and holder (1937–1938) of a Bursary under the National Research Council of Canada, at Dalhousie University. Present address National Research Council, Ottawa.

⁴ Associate Professor of Chemistry.

The introduction of a double bond in the aldehyde end, however, resulted in a marked increase in reaction rate with no measurable change in activation energy. This increase, moreover, appeared to be singularly independent of the nature of the group furnishing the unsaturation provided that the latter was situated at a given distance from the breaking bonds. For example the crotonylidene, furfurylidene, and benzylidene esters all have identical decomposition velocities at all temperatures (6, 8). This effect of unsaturation is being further investigated in the light of an earlier hypothesis (2) regarding the ease of energy distribution within a complex molecule.

The present paper deals with the decomposition of a somewhat different ester; viz., glyoxal-acetate. As before, the reaction is homogeneous and first order. It is complete in the direction of decomposition—the pressure increasing 300%. It has, however, an appreciably higher activation energy than the simpler esters of the series and a temperature independent factor approaching that to be expected (viz. 10^{13} to 10^{15}) for unimolecular gas reactions.

Experimental

The ester was made through glyoxal sulphate from tetrachlorethane and fuming sulphuric acid.

The sulphate was prepared by slowly adding tetrachlorethane to vigorously stirred 65% oleum held at a temperature of 50° to 60° C. The oleum contained a trace of mercurous sulphate as a catalyst. The resulting mixture was cooled and the precipitated glyoxal sulphate was filtered off through glass wool and washed with tetrachlorethane.

The sulphate was then refluxed with a mixture of acetic acid and acetic anhydride. (External cooling is necessary at this point as the reaction is rather violent.) The final product (glyoxal tetra-acetate) was obtained by pouring the reaction mixture into ice water, filtering, and crystallizing from alcohol. Two recrystallizations gave a perfectly white product which melted sharply at 103° C.

Two independent preparations of the ester were used in the runs listed in Table I.

The reaction rate measurements were carried out in apparatus of the type already described. Three different operators using two different pieces of apparatus obtained the data submitted. The high melting point of this ester made it more convenient to pack the crystals into small glass thimbles rather than to fill bulbs with the liquid as had been done previously.

The final pressures showed a greater drift than is usually found for the diacetate esters. This is probably due to a heterogeneous decomposition of the glyoxal, as the effect is practically independent of temperature and the surface of the reaction chamber becomes rapidly coated with a dark film. However the final pressure obtained by extrapolating back to zero time was always found to agree within a few per cent with that calculated ($3P_0$), so that no difficulty was experienced in obtaining satisfactory rate constants by plotting $\log 2P_0/3P_0 - P$ against time.

Results

The data are summarized in Table I which is self-explanatory. Initial pressures are not listed as they were varied between 4 and 40 cm. without producing any change in specific reaction rate.

In Fig. 1 the negative logarithms of the mean velocity constants are plotted against the reciprocals of the absolute temperature. The broken lines in the figure represent the decomposition of ethylidene diacetate (1) (upper

TABLE I
SUMMARY OF REACTION VELOCITY DATA

Temp., °Abs.	$k \times 10^4$, sec. ⁻¹	$-\log k$	$1/T \times 10^3$
538.3	2.06	3.668	1.856
538.3	2.17		
539.1	2.19		
539.1	2.19		
543.6	3.07	3.510	1.841
543.3	3.12		
543.3	3.10		
543.3	3.10		
543.3	3.20		
543.3	3.03		
543.3	3.20		
543.3	3.20		
543.3	2.76	3.323	1.824
548.0	3.96		
548.0	3.96		
548.6	4.70		
548.6	5.07		
548.6	4.11		
548.6	5.56		
548.6	4.68		
548.6	5.19		
548.6	5.23	3.275	1.813
551.5	5.10		
551.5	6.02		
551.5	4.88		
551.5	5.28	3.101	1.795
557.0	7.06		
557.0	8.03		
557.0	7.79		
557.0	8.83	3.060	1.787
559.4	8.90		
559.4	8.31		
559.4	8.75		
559.4	8.85	2.807	1.760
568.0	15.6		
568.0	16.2		
568.0	15.8		
568.0	13.9		
568.0	16.7	2.740	1.752
570.9	18.2		
570.9	18.2		
570.9	18.0	2.466	1.715
583.0	40.7		
583.0	41.0		
583.0	40.6		

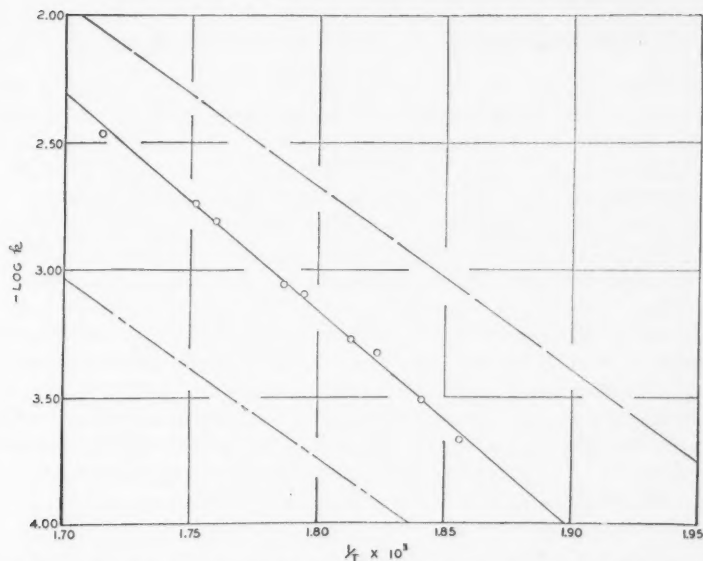


FIG. 1. $-\log k$ plotted against $1/T$. — — — Ethylidene diacetate, $\circ \circ \circ$ Glyoxal tetra-acetate, — · — Methylene diacetate.

line) and methylene diacetate (4) (lower line) and are included for purposes of comparison. The corresponding equations are as follows:

$$\begin{aligned} \text{Methylene diacetate} \quad k &= 1.7 \times 10^9 e^{-33000/RT} \\ \text{Glyoxal tetra-acetate} \quad k &= 1.8 \times 10^{12} e^{-39200/RT} \\ \text{Ethylidene diacetate} \quad k &= 2.0 \times 10^{10} e^{-33000/RT} \end{aligned}$$

It is to be noted that in the case of the most complex ester, the tetra-acetate both the activation energy and the temperature independent factor of the rate constant are substantially greater than for the others. In this respect it resembles paraldehyde (3) ($k = 1.4 \times 10^{15} e^{-44160/RT}$), which also breaks into three parts, more nearly than do the diacetates, which simply break in two. It is to be expected that these ester and paraldehyde decompositions would be very similar as each involves the breaking of carbon-to-oxygen bonds. Discussion of these results is reserved until more data have been obtained.

References

1. COFFIN, C. C. Can. J. Research, 5 : 636-647. 1931.
2. COFFIN, C. C. Can. J. Research, 6 : 417-427. 1932.
3. COFFIN, C. C. Can. J. Research, 7 : 75-80. 1932.
4. COFFIN, C. C. and BEAZLEY, W. B. Can. J. Research, 15 : 229-236. 1937.
5. COFFIN, C. C., DACEY, J. R., and PARLEE, N. A. D. Can. J. Research, 15 : 247-253. 1937.
6. DACEY, J. R. and COFFIN, C. C. Can. J. Research, 15 : 260-263. 1937.
7. DACEY, J. R. and COFFIN, C. C. J. Chem. Phys. 7 : 315-317. 1939.
8. PARLEE, N. A. D., ARNELL, J. C., and COFFIN, C. C. Can. J. Research, 18 : 223-230. 1940.
9. PARLEE, N. A. D., DACEY, J. R., and COFFIN, C. C. Can. J. Research, 15 : 254-259. 1937.

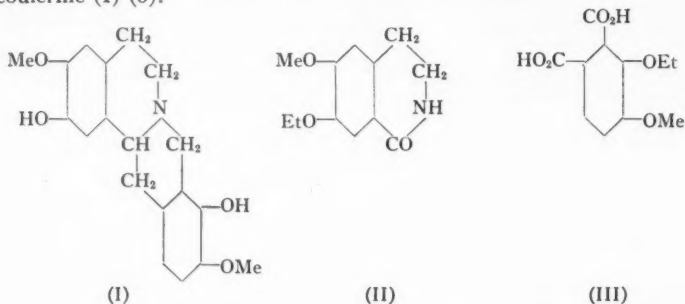
THE ALKALOIDS OF FUMARIACEOUS PLANTS

XXX. AUROTENSINE¹BY RICHARD H. F. MANSKE²

Abstract

The alkaloid aurotensine is shown to have the same constitution as scoulerine. It is not the optical antipode nor the *dl*-form of the latter, but an addition compound of the *l*- and the *dl*-forms. Scoulerine diethyl ether and the mono-ethyl ethers of corypalmine and of isocorypalmine have been obtained in crystalline condition, thus facilitating the unambiguous characterization of the alkaloids.

The author has recorded the isolation of an alkaloid, aurotensine, from *Corydalis aurea* (2), from *C. ochotensis* (6), and from *Glaucium flavum* (5). Its empirical formula is $C_{19}H_{21}O_4N$, and it contains two methoxyl groups and two hydroxyl groups, which latter may be methylated with diazomethane. The resulting dimethyl ether on appropriate purification yields *l*-tetrahydropalmatine (7). It is therefore to be concluded that aurotensine is isomeric with scoulerine (I) (3).



The constitution of the latter alkaloid has been elucidated by Gadamer, Späth, and Mosettig (1). The author has repeated the degradation procedure and isolated the two fragments, 6-methoxy-7-ethoxy-1-keto-1 : 2 : 3 : 4-tetrahydro-isoquinoline (II) and 3-ethoxy-4-methoxy-phthalic acid (III) characterized as its ethyl-imide, thus confirming the results of Gadamer and co-workers. The intermediate diethyl ether and its hydrochloride have been obtained in crystalline form.

Degradation of aurotensine by the same procedure was expected to yield a corydaldine and a phthalic acid, at least one of which would be different from those obtained from scoulerine. Neither the intermediate diethyl ether nor its hydrochloride could be obtained in crystalline condition, but oxidation yielded the same two substances, (II) and (III), that were obtained from

¹ Manuscript received July 13, 1940.

Contribution from the Division of Chemistry, National Research Laboratories, Ottawa, Canada. Issued as N.R.C. No. 958.

² Chemist.

scoulerine. It is therefore concluded that formula (I) is also that of aurotensine.

This leaves unexplained why aurotensine and scoulerine are not identical in spite of the fact that *l*-tetrahydro-palmatine has been obtained from both alkaloids on methylation. It has not been possible to convert one alkaloid into the other. A supersaturated solution of one base is not induced to crystallize when seeded with the other. The optical activities of the two alkaloids however are considerably different. Aurotensine has $[\alpha]_D - 69.9^\circ$ a figure that is much less than that for bases of the tetrahydro-protoberberine type, which have values of the order of 200° to 300° . If it be assumed that aurotensine consists of a compound composed of one molecule of *dl*-scoulerine and one of *l*-scoulerine, the value of -69.9° is reasonable. This assumption further explains the fact that *l*-tetrahydro-palmatine can be isolated from methylated aurotensine but that the ethylated bases, being more difficult to separate, remained amorphous. Sufficient material was not available to attempt the isolation of the pure *l*- and *dl*-ethers of aurotensine.

The successful crystallization of scoulerine diethyl ether has made it a useful derivative for characterizing scoulerine. It seemed therefore desirable to attempt to crystallize the ethyl ethers of corypalmine and of isocorypalmine so that these alkaloids could be unambiguously characterized. This has been done. The substances melt at 120°C.^* and 82°C. respectively. Both ethers yield sparingly soluble hydrochlorides, thus facilitating their purification. They have been oxidized to the corresponding corydaldines, thus confirming the constitutions assigned to them by Späth and Mosettig (9) and by Gadamer, Späth, and Mosettig (1).

Experimental

Ethylation of Scoulerine and its Degradation

A suspension of scoulerine in absolute ethanol was treated with an excess of an ethereal solution of diazoethane. The evolution of nitrogen proceeded briskly. After the solution had stood in the refrigerator for 24 hr. the solvents were boiled off and the residue was dissolved in hot dilute hydrochloric acid. The filtered solution on cooling deposited a sparingly soluble hydrochloride. This was filtered off, suspended in water and ether, and shaken with an excess of aqueous potassium hydroxide. The washed ether solution was evaporated to a small volume and the base thus obtained recrystallized from dry ether, in which it is only sparingly soluble. Scoulerine diethyl ether as thus obtained consists of colourless fine prisms that melt sharply at 155°C.

For the purpose of oxidizing this base the following procedure was employed. It is based on the work of Gadamer and co-workers (1) except that a larger proportion of permanganate was found to be advantageous. A solution of 1.3 gm. of the diethyl ether in dilute hydrochloric acid was treated with an aqueous solution of sodium bicarbonate until the incipient turbidity was just permanent. The solution was then cooled to 0°C. and a cold solution

* All melting points are corrected.

of 2.35 gm. of potassium permanganate added at once. When the permanganate had been reduced (about one hour), the mixture was heated and filtered. The cooled filtrate was exhausted with ether and the combined extracts evaporated to dryness. The residue was extracted with several successive portions of hot water and the filtered extract again exhausted with ether. The residue from these extracts, which crystallized at once, was washed with a little ether and sublimed *in vacuo*. The brilliant stout prisms thus obtained melted sharply at 195° C. and are evidently identical with 6-methoxy-7-ethoxy-1-keto-1 : 2 : 3 : 4-tetrahydro-isoquinoline (1).

The aqueous solution remaining from the first ether extraction was heated to expel the ether and treated with potassium permanganate until the colour was permanent for two hours. A stream of sulphur dioxide was passed in until the solution was clear. The solution was then evaporated to a small volume. An excess of hydrochloric acid was added and the solution repeatedly extracted with ether. The residue from the extract was dissolved in water and an excess of calcium acetate added. The filtrate from the calcium oxalate was acidified with hydrochloric acid and again extracted with ether. The acetic acid was removed from the extract by repeated evaporation with ethanol and the residue treated with ethanolic ethylamine and distilled *in vacuo*. The crystalline distillate was washed with cold methanol and recrystallized from the hot solvent. The 4-methoxy-5-ethoxy-N-ethyl-phthalimide thus obtained melted sharply at 205° C. (8).

The methanolic washings were evaporated to dryness and the residue extracted with several successive portions of boiling hexane. The concentrated extract was treated with dry ether until the turbidity had disappeared. The crystals that then separated melted at 82° to 84° C. The melting point of 3-ethoxy-4-methoxy-N-ethyl-phthalimide is given as 84 to 85° (?corr.) (1), and the author's substance is undoubtedly the same. However, when it was recrystallized twice more from hexane-ether it was obtained in brilliant prisms that melt sharply at 90° C. In admixture with N-ethyl-hemipinimide, which also melts at 90° C., it began to sinter at 75° C. and was completely liquid at 80° C.

Degradation of Aurotensine

The diethyl ether of aurotensine was prepared as in the case of scoulerine, but owing to the more sparing solubility of aurotensine it was necessary to use more diazoethane and leave the solution for several days. The non-phenolic product in ether solution was washed with aqueous potassium hydroxide. It could not be obtained crystalline in contact with ether or methanol, and the hydrochloride separated as an oil from a concentrated aqueous solution.

The oxidation was carried out exactly as in the above case. There was used 2.6 gm. of diethyl ether and 4.7 gm. of potassium permanganate. The corydaldine melted at 195° C. either alone or in admixture with the above specimen. The two N-ethyl-imides had the correct melting points either alone or in admixture with the corresponding authentic specimens.

Ethylation of Corypalmine and of Isocorypalmine (4)

Owing to the sparing solubility of these alkaloids in ethanol it was necessary to add small quantities of diazoethane from day to day until the alkaloids had completely dissolved. The non-phenolic fraction was then isolated by adding an excess of aqueous potassium hydroxide to a dilute hydrochloric acid solution of the bases. The precipitates were taken up in ether and the washed ether solution evaporated to a small volume. Both hydrochlorides are sparingly soluble in water, that of the ethyl ether of isocorypalmine melting at 230° C. to a red liquid with previous sintering.

Corypalmine ethyl ether was recrystallized twice from dry ether. It was obtained in colourless fine prisms that melt sharply at 120° C.

Isocorypalmine ethyl ether was recrystallized from dry ether but it was more soluble than the above-mentioned compound. It consists of colourless needles that melt not quite sharply at 82° C. with a noticeable evolution of vapours, particularly at a higher temperature. It is probable that some water of crystallization is present in this ether. An attempt to recrystallize it from benzene or benzene-hexane was not successful owing to its great solubility in the former solvent.

The oxidation of these ethers was carried out as in the case of scoulerine diethyl ether. Corypalmine ethyl ether yielded 6-ethoxy-7-methoxy-1-keto-1 : 2 : 3 : 4-tetrahydro-isoquinoline melting at 175° C. (8). Isocorypalmine yielded the same corydaldine that was obtained from scoulerine.

References

1. GADAMER, J., SPÄTH, E., and MOSETTIG, E. Arch. Pharm. 265 : 675-684. 1927.
2. MANSKE, R. H. F. Can. J. Research, 9 : 436-442. 1933.
3. MANSKE, R. H. F. Can. J. Research, B, 14 : 347-353. 1936.
4. MANSKE, R. H. F. Can. J. Research, B, 17 : 95-98. 1939.
5. MANSKE, R. H. F. Can. J. Research, B, 17 : 399-403. 1939.
6. MANSKE, R. H. F. Can. J. Research, B, 18 : 75-79. 1940.
7. MANSKE, R. H. F. and MILLER, M. R. Can. J. Research, B, 16 : 153-157. 1938.
8. SPÄTH, E. and DOBROWSKY, A. Ber. 58 : 1274-1284. 1925.
9. SPÄTH, E. and MOSETTIG, E. Ber. 58 : 2133-2135. 1925.



CANADIAN JOURNAL OF RESEARCH

VOLUME 18

1940

SECTION B



CANADA

Published by the
**NATIONAL
RESEARCH COUNCIL**
of CANADA



Section B
INDEX TO VOLUME 18
Authors

- Arnell, J. C.**—See Parlee, N. A. D.
- Arnell, J. C., Dacey, J. R., and Coffin, C. C.**—Studies on homogeneous first order gas reactions. XII. The decomposition of glyoxal tetra-acetate, 410.
- Ashley, R. W.**—See Campbell, A. N.
- Brawn, J. S.**—See Heddle, R. D.
- Campbell, A. N., and Ashley, R. W.**—The alloys of aluminium and lead, 281.
- Campbell, W. B.**—See Morrison, J. L.
- Coffin, C. C.**—Platinized glass as a laboratory substitute for massive platinum, 318.
- Coffin, C. C.**—See Arnell, J. C., Parlee, N. A. D.
- Collier, H. B.**—A small-scale electro dialysis, cell, 252.
The problem of plastein formation.
I. The formation of a plastein by papain, 255.
II. The chemical changes involved in plastein formation by papain and by pepsin, 272.
III. A note on the complexity of peptic plastein in urea solution, 305.
Enzyme inhibition by derivatives of phenothiazine and of sulphanilamide, 345.
- Dacey, J. R.**—See Arnell, J. C.
- Demers, P.**—See Lortie, L.
- Donald, R. M.**—The fractionation of Turner Valley crude oils using Stedman columns, 12.
- Dorland, R. M. and Hibbert, H.**—Formic acid as a solvent for ozonization investigations, 30.
- Findlay, R. A.**—See Marshall, M. J.
- Finlay, G. R.**—See Walker, O. J.
- Folkins, H. O.**—See Steacie, E. W. R.
- Froman, D. K. and McFarlane, W. D.**—A photoelectric colorimeter-fluorimeter, 240.
- Giguère, P. A. and Maass, O.**—Solid solutions of hydrogen peroxide and water, 66.
The heterogeneous catalytic decomposition of hydrogen peroxide in heavy water, 84.
Vapour pressures and boiling points of binary mixtures of hydrogen peroxide and water, 181.
- Gordon, W. E. and Spinks, J. W. T.**—Nitroxyl perchlorate, 358.
- Hamilton, J. D.**—Gelation phenomena in wheat flour films, 194.
- Heatley, A. H.**—A note on the velocity distribution of gaseous molecules; and a table for obtaining values of the error function complement, 123.
- Heddle, R. D. and Brawn, J. S.**—The phosphorus and iodine contents of British Columbia fish oils, 386.
- Hibbert, H.**—See Dorland, R. M.
- Holder, C. H. and Maass, O.**—Solubility measurements in the region of the critical temperature, 293.

- Johnson, L. R.**—See Thorvaldson, T.
- Lathe, F. E.**—The determination of the metals of the platinum group in nickel ores and concentrates, 333.
- Lortie, L. and Demers, P.**—Études physico-chimiques sur les carbonates alcalins.
I. Recherches sur l'activité des ions-hydrogène dans les solutions aqueuses de carbonates alcalins, 160.
II. Calcul des coefficients d'activité des carbonates de sodium et de potassium, en solution aqueuse, 373.
- Maass, O.**—See Giguère, P. A., Holder, C. H., Mason, S. G., Morrison, J. L., Naldrett, S. N., Ross, A. S.
- McCutcheon, J. W.**—Linolenic acid and its isomers, 231.
- McFarlane, W. D.**—See Froman, D. K., Parker, W. E.
- McGinnis, N. A.**—See McRae, J. A.
- McRae, J. A.**—See Marion, L.
- McRae, J. A. and McGinnis, N. A.**—Derivatives of substituted succinic acids. IV. The action of alkaline sodium hypobromite on some α -alkyl- α' -arylsuccinamides, 90.
- Manske, R. H. F.**—The alkaloids of fumariaceous plants.
XXIV. *Corydalis ochotensis* Turcz., 75.
XXV. *Corydalis pallida* Pers., 80.
XXVI. *Corydalis claviculata* (L.) DC., 97.
XXVII. A new alkaloid, cheilanthifoline, and its constitution, 100.
XXVIII. *Corydalis nobilis* Pers., 288.
XXX. Aurotensine, 414.
- Marion, L.**—The reaction of polystyrenes with bromine, 309.
- Marion, L. and McRae, J. A.**—Naphthalene derivatives from substituted γ -phenylcrotonic esters, 265.
- Marshall, M. J. and Findlay, R. A.**—The equilibrium pressures of oxygen adsorbed on activated charcoal, 35.
- Mason, S. G. and Maass, O.**—Measurement of viscosity in the critical region. Ethylene, 128.
- Mason, S. G., Naldrett, S. N., and Maass, O.**—A study of the coexistence of the liquid and gaseous states of aggregation in the critical temperature region. Ethane, 103.
- Morrison, J. L., Campbell, W. B., and Maass, O.**—The heats of adsorption and wetting of mercerized celluloses by sodium hydroxide solutions, water, and methyl alcohol, 168.
- Mungen, R. and Spinks, J. W. T.**—The bromine sensitized photodecomposition of ozone, 363.
- Naldrett, S. N.**—See Mason, S. G.
- Naldrett, S. N. and Maass, O.**—A study of the coexistence of the liquid and gaseous states of aggregation in the critical temperature region, 118.
The viscosity of carbon dioxide in the critical region, 322.
- Parker, W. E. and McFarlane, W. D.**—A proposed modification of Emmerie's iron-dipyridyl method for determining the tocopherol content of oils, 405.
- Parlee, N. A. D., Arnell, J. C., and Coffin, C. C.**—Studies on homogeneous first order gas reactions. XI. The decomposition of benzylidene diacetate, *o*-chlorobenzylidene diacetate, and benzylidene dibutyrate, 223.
- Potvin, R.**—See Steacie, E. W. R.

— III —

Ross, A. S. and Maass, O.—The density of gaseous chlorine, 55.

Shane, G.—See Steacie, E. W. R.

Spinks, J. W. T.—See Gordon, W. E., Mungen, R., and Watson, L. M.

Steacie, E. W. R.—The quenching of mercury resonance radiation by ethylene, 44.

Steacie, E. W. R. and Folkins, H. O.—The kinetics of the thermal decompositions of the lower paraffins. V. The nitric oxide inhibited decomposition of *n*-butane, 1.

Steacie, E. W. R. and Potvin, R.—Cadmium photosensitized reactions of ethylene, 47.

Steacie, E. W. R. and Shane, G.—The kinetics of the decomposition reactions of the lower paraffins.

VI. Ethane, 203.

VII. The nitric oxide inhibited decomposition of ethane, 351.

Stonestreet, G. O. and Wright, G. F.—Microchemical technique. IV. The microdetermination of mercury and halogen in organomercuric halides, 246.

Tapp, J. S.—The construction and operation of a simple automatic multiple burette, 217.

Thorvaldson, T. and Johnson, L. R.—The selenium content of Saskatchewan wheat, 138.

Walker, O. J. and Finlay, G. R.—The determination of small amounts of fluorine in water, 151.

Watson, L. M. and Spinks, J. W. T.—The separation and identification of the compounds present in a Turner Valley crude oil, 388.

Wright, G. F.—See Stonestreet, G. O.

SECTION B
INDEX TO VOLUME 18

Subjects

- Absorption spectra**, Ultraviolet, of Turner valley crude oil containing aromatics, 25.
- 1-Acetamino-2-methyl-4-nitronaphthalene**, 269.
- Activity coefficients**
of binary mixtures of hydrogen peroxide and water, 190.
of potassium and sodium carbonates in aqueous solution, 373.
- Adsorption**
Equilibrium pressures of oxygen adsorbed on activated charcoal, 35.
Heat of, of sodium hydroxide solutions, water, and methyl alcohol by mercerized celluloses, 168.
- Alberta waters**, Determination of fluorine in, 151.
- Alkaline carbonates**
pH of solutions of, 160, 164.
See Potassium and sodium carbonates.
- Alkaloid F13**, See Cheilanthifoline.
- Alkaloid F36** (sinactine), Oxidation of, 100.
- Alkaloid F48** (ochotensimine), from *Corydalis ochotensis*, 76.
- Alkaloid F49** from *Corydalis ochotensis*, 78.
- Alkaloid F50** (capaurimine) from *Corydalis pallida*, 82.
- Alkaloid F51** from *Corydalis pallida*, 82.
- Alkaloid F52** from *Corydalis claviculata*, 99.
- Alkaloid F53** from *Corydalis nobilis*, 290.
- Alkaloid F54** from *Corydalis nobilis*, 292.
- Alkaloid F55** from *Corydalis nobilis*, 291.
- Alkaloids of fumariaceous plants**,
XXIV. *Corydalis ochotensis* Turcz., 75.
XXV. *Corydalis pallida* Pers., 80.
XXVI. *Corydalis claviculata* (L.) DC., 97.
XXVII. A new alkaloid, cheilanthifoline, and its constitution, 100.
XXVIII. *Corydalis nobilis* Pers., 288.
XXX. *Aurotensine*, 414.
- α -Alkyl- α' -arylsuccinamides**, Action of alkaline sodium hypobromite on, 90.
- Alloys of aluminium and lead**, 281.
- Aluminium and lead**, Alloys of, 281.
- 1-Amino-2-methyl-naphthalene**, 268.
- 1-Amino-2-methyl-4-nitro-naphthalene**, 269.
- Analysis**
Microdetermination of mercury and halogen in organomercuric halides, 246.
Proposed modification of Emmerie's iron-dipyridyl method for determining toopherol content of oils, 405.
- Anaphylactic reaction**, in guinea-pigs by plastein in urea, 305.
- Apparatus**
for microdetermination of halogen, 249.
Photoelectric colorimeter-fluorimeter, 240.
Simple, automatic, multiple burette, 217.
Small-scale electroanalysis cell, 252.
Use of platinized glass in construction of, 318.
- Aromatic hydrocarbons**, Physical properties of, 28, 403.
- Aurotensine**
Degradation of, 416.
from *Corydalis ochotensis*, 78.
- Benzoyl hydrogen peroxide**, Reaction with polystyrenes, 311.
- Benzylidene diacetate**, Thermal decomposition of, 223.
- Bicuculline**, Isolation of, from *Corydalis nobilis*, 290.
- Boiling points** of binary mixtures of hydrogen peroxide and water, 181.
- Bromine**
or chlorine and mercury in organomercurials, simultaneous microdetermination of, 246.
Reaction with
di-indene, 311, 313.
polystyrenes, 309.
-sensitized photodecomposition of ozone, 363.

Bromine oxide, Formation of, in bromine sensitized photodecomposition of ozone, 363.

Burette, Simple automatic multiple, 217.

n-Butane, Nitric oxide inhibited decomposition of, 1.

Cadmium photosensitized reactions of ethylene, 47.

Capauridine from *Corydalis pallida*, 81.

Capaurimine (F50) from *Corydalis pallida*, 82.

Capaurine from *Corydalis pallida*, 81.

Carbon dioxide, Viscosity of, in the critical region, 322.

Catalase, Mammalian, Inhibition of, by phenothiazine derivatives, 346.

Catalytic decomposition of hydrogen peroxide on gold and on glass, in heavy water, 84.

Cellulose(s),

Mercurized, Heats of adsorption and wetting of, 168.

Physical structure of, 178.

Charcoal, Activated coconut, Equilibrium pressure of oxygen adsorbed on, 35.

Cheilanthisoline (F13) from *Corydalis cheilanthisolia*, 100.

Cheilanthisoline O-ethyl ether, Oxidation of, 102.

Chemisorption of oxygen on activated charcoal, 35.

Chlorine,

Gaseous, Density of, 55.

or bromine and mercury in organomercurials, Simultaneous microdetermination of, 246.

o-Chlorobenzylidene diacetate, Thermal decomposition of, 223.

Coexistence curve of

ethane, 113.

ethylene, 119.

Colorimeter-fluorimeter, A photoelectric, 240.

Colorimetric method for determination of fluorine in water, 151.

Corlumine, isolation of, from *Corydalis nobilis*, 290.

Corydalis cheilanthisolia, Alkaloids from 100.

Corydalis claviculata, Alkaloids from 97.

Corydalis nobilis, Alkaloids from, 288.

Corydalis ochotensis, Alkaloids from, 75.

Corydalis pallida, Alkaloids from 80.

Corypalline from *Corydalis pallida*, 83.

Corypalmine, Ethylation of, 417.

Corytuberine, from *Corydalis nobilis*, 292.

Cottons

Heat of adsorption of sodium hydroxide, by, 170.

Heats of wetting of, by water and methyl alcohol, 171.

Critical dispersion temperature, (critical region), 118.

Critical temperature region

Coexistence of liquid and gaseous states of aggregation in, ethane, 103.

ethylene, 118.

Ethylene, Measurement of viscosity in the, 128.

Solubility measurements in, 293.

Viscosity of carbon dioxide in, 322.

Crotonic esters, γ -Phenyl-, Substituted, Naphthalene derivatives from, 263.

Crude oil, Turner Valley, Distillation of, 12, 388.

Cryptocavine from *Corydalis ochotensis*, 78.

Cryptopine, from *Corydalis nobilis*, 291.

Cularine from *Corydalis claviculata*, 98.

Cytochrome oxidase, See Oxidase.

Decomposition reactions, See Thermal decomposition.

Density of gaseous chlorine, 55.

Density-viscosity-temperature relations of carbon dioxide in critical region, 326, 327.

Deuterium oxide, Heterogeneous catalytic decomposition of hydrogen peroxide in, 84.

Deuterium peroxide and hydrogen peroxide, Relative stability of, to catalysts, 84.

Diethyl malonate, Condensation with phenylacetone, 267.

Di-indene, Reaction of, with bromine, 311, 313.

Distillation of Turner Valley crude oils using Stedman columns, 12, 388.

Electrodialysis cell for removing electrolytes from colloidal solutions, 252.

Emmerie's iron-dipyridyl method for determining tocopherol content of oils, Proposed modification of, 405.

Enzymatic hydrolysis of plasteins, 272.

Enzymatic synthesis of plasteins, 255, 272, 305.

Enzyme(s)

Chemical changes in plastein formation by papain and by pepsin, 272.

Formation of a plastein by papain, 255.

inhibition by phenothiazine and sulphanilamide derivatives, 345.

inhibitors, Effect of, on plastein formation by papain, 260.

Ethane

Kinetics of the

thermal decomposition of, 203.

nitric oxide inhibited thermal decomposition of, 351.

Solubility of hexachloroethane in, in region of critical temperature, 293.

Study of coexistence of liquid and gaseous states of, in critical temperature region, 103.

Ethyl acetate as an ozonization solvent, 31.

Ethyl α -carbethoxy- β -methyl- γ -phenyl- Δ^2 -butenoate, 267.

Ethyl cyanoacetate, Condensation with phenylacetone, 271.

Ethylene

and ethylene-hydrogen mixtures, Cadmium photosensitized reactions of, 47.

Measurement of viscosity in the critical region, 128.

Quenching of mercury resonance radiation by, 44.

Study of coexistence of liquid and gaseous states of, in critical temperature region, 118.

Ethyl linolenate, Physical properties of, 235, 236.

N-Ethyl-metahemipinimide, 101.

Films

Wheat flour, Gelation phenomena in, 194.

Fish oils

British Columbia, Phosphorus and iodine contents of, 386.

Flour films

Wheat, Gelation phenomena in, 194.

Flow of liquids, Controlled by simple automatic multiple burette, 217.

Fluorimeter, Photoelectric colorimeter-, 240.

Fluorine in Alberta waters, Determination of, by colorimetric method, 153, titration method, 152.

Formic acid as a solvent for ozonization investigations, 30.

Comparison with ethyl acetate, 31.

Fractionation of Turner Valley crude oils using Stedman columns, 12, 388.

Fumariaceous plants, Alkaloids of, 75, 80, 97, 100, 288, 414.

Fumaric acid from *Corydalis ochotensis*, 79.

Gaseous molecules, Velocity distribution of, 123.

Gas reactions

Studies on homogeneous first order

XI. The decomposition of benzylidene diacetate, *o*-chlorobenzylidene diacetate, and benzylidene dibutyrate, 223.

XII. The decomposition of glyoxal tetra-acetate, 410.

Gelation phenomena in wheat flour films, 194.

Glass

Catalytic decomposition of hydrogen peroxide on, in heavy water, 84.

Platinized, as a laboratory substitute for massive platinum, 318.

Glyoxal tetra-acetate, Decomposition of, 410.

Gold

Catalytic decomposition of hydrogen peroxide on, in heavy water, 87.

Detection of platinum metals in assaying for, 335.

Halogen, Microdetermination of, in organo-mercuric halides, 246.

Heat

- of adsorption of sodium hydroxide by mercerized and standard cottons, 170.
- of mercerization, 168.
- of vaporization, Latent, of hydrogen-peroxide-water mixtures, 189.
- of wetting of mercerized cottons by water and methyl alcohol, 171.

Hexachloroethane, Solubility of, in ethane in region of critical temperature, 293.

Hydrocarbons, Physical properties of,

- Aromatic, 29, 403.
- Naphthenic, 28, 403.
- Paraffinic, 27, 402.

Hydrogen-ethylene mixtures, Cadmium photosensitized reactions of, 47.

Hydrogen ion concentration

- in sodium and potassium carbonate solutions at 25° C., 160, 164.
- Optimum, for plastein formation, by papain, 258.

Hydrogen peroxide

- and water, Solid solution of, 66.
- and water, Vapour pressures and boiling points of binary mixtures of, 181.
- Heterogeneous catalytic decomposition of, in heavy water, 84.
- on glass, 84.
- on gold, 87.

Hydrolysis, Enzymatic, of plasteins, 272.

p-Hydroxylaminobenzenesulphonamide, Inhibition of mammalian catalase and cytochrome oxidase by, 345.

Iodine and phosphorus contents of British Columbia fish oils, 386.

Iridium, Determination of, in nickel ores and concentrates, 341.

Iron-dipyridyl method for determining tocopherol content of oils, Emmerie's, Proposed modification of, 405.

Isocorypalmine, Ethylation of, 417.

d-Isocorypalmine from *Corydalis nobilis*, 290.

Isomerism

- Linolenic acid and its isomers, 231.

Isoquinoline, 6-Methoxy-7-ethoxy-1-keto-1 : 2 : 3 : 4-tetrahydro-, 100.

Kinetics of the thermal decomposition reactions of the lower paraffins.

- V. The nitric oxide inhibited decomposition of *n*-butane, 1.
- VI. Ethane, 203.
- VII. The nitric oxide inhibited decomposition of ethane, 351.

Latent heat of vaporization of binary mixtures of hydrogen peroxide and water, 189.

Lead, Alloys of aluminium and, 281.

Linolenic acid and its isomers, 231.

Liquids, Controlled flow of, by simple automatic, multiple burette, 217.

Maleic acid, Ozonization of,
in ethyl acetate, 32
in formic acid, 32

Maltol from *Corydalis ochotensis*, 79.

Mercerization, Heat of, 168.

Mercerized celluloses, Heats of adsorption and wetting of, by sodium hydroxide solutions, water, and methyl alcohol, 168.

Mercury

- in organomercurials, Microdetermination of chlorine or bromine and, 246.
- resonance radiation, The quenching of, by ethylene, 44.

Methyl alcohol, Heat of wetting of mercerized cottons by, 171.

2-Methyl-4-amino-naphthalene, 269.

3-Methyl-1-hydroxy-2-naphthoic acid, 270.

3-Methyl-1-hydroxy-2-naphthoic nitrile, 271.

3-Methyl-1-naphthol, 270.

2-Methyl-4-nitro-naphthalene, 269.

Microchemical technique

- IV. The microdetermination of mercury and halogen in organomercuric halides, 246.

Molecules, Gaseous, Velocity distribution of, 123.

Naphthalene

- 1-Acetamino-2-methyl-4 nitro-, 269.
- 1-Amino-2-methyl-, 268.
- 1-Amino-2 methyl-4-nitro-, 269.
- 2-Methyl-4-amino-, 269.
- 2-Methyl-4-nitro-, 269.
- 1-Nitro-2 methyl-, 268.

Naphthalene derivatives from substituted γ -phenylcrotonic esters, 265.

- Naphthenic hydrocarbons**, Physical properties of, 28, 403.
- Naphthoic acid, 3-Methyl-1-hydroxy-**, 268, 270.
- 2-Naphthoic nitrile, 3-Methyl-1-hydroxy-**, 271.
- 1-Naphthol, 3-Methyl-**, 270.
- Nickel ores** and concentrates, Determination of metals of platinum group in, 333.
- Nitric acid** separation of metals of platinum group in nickel ores, 339.
- Nitric oxide** inhibited thermal decomposition of
n-butane, 1.
ethane, 351.
- 1-Nitro-2-methyl-naphthalene**, 268.
- Nitroxyl perchlorate**, Preparation, analysis, and properties of, 358.
- Ochotensimine (F48)** from *Corydalis ochotensis*, 76.
- Ochotensine (F17)** from *Corydalis ochotensis*, 77.
- Oils**, British Columbia fish, Phosphorus and iodine contents of, 386.
- Oils**, Proposed modification of Emmerie's iron-dipyridyl method for determining tocopherol content of, 405.
- Oils**, Turner Valley crude. Fractionation of, using Stedman columns, 12, 388.
- Organomercuric halides**, Microdetermination of mercury and halogen in, 246.
- Osmium**, Determination of, in nickel ores and concentrates, 338.
- Oxidase**, Cytochrome, Inhibition of, by phenothiazine derivatives, 347.
- Oxidation of**
Alkaloid F36 (sinactine), 101.
cheilanthifoline O-ethyl ether, 102.
polystyrenes, 310.
- Oxygen** adsorbed on activated charcoal, Equilibrium pressures of, 35.
- Ozone**, Bromine photosensitized decomposition of, 363.
- Ozonization** investigations, Formic acid as a solvent for, 30.
- Palladium**, Determination of, in nickel ores and concentrates, 341.
- Papain**
Chemical changes in plastein formation by, and by pepsin, 272.
Formation of a plastein by, 255.
Synthesis of plastein by, 273.
- Papain hydrolysis** of papain plastein, 274.
- Paraffinic compounds**, Properties of, 27, 402.
- Paraffins**, Lower
Kinetics of the thermal decomposition of,
V. Nitric oxide inhibited decomposition of *n*-butane, 1.
VI. Ethane, 203.
VII. Nitric oxide inhibited decomposition of ethane, 351.
- Pepsin**, Chemical changes in plastein formation by, 272.
- Peptic hydrolysis of**
papain plastein, 274.
peptic plastein, 275.
typical proteins, 276.
- Peptic plastein**, 275
in urea solution, Complexity of, 305.
Peptic hydrolysis of, 275.
- Phase rule** diagram of the system water-hydrogen-peroxide, 69.
- Phenothiazine** and sulphanilamide, Enzyme inhibition by derivatives of, 345.
- Phenylacetone**
condensation with
diethyl malonate, 267.
ethyl cyanoacetate, 271.
- γ -Phenylcrotonic esters, Substituted**, Naphthalene derivatives from, 265.
- Phosphorus** and iodine contents of British Columbia fish oils, 386.
- Photodecomposition** of ozone, Bromine sensitized, 363.
- Photoelectric colorimeter-fluorimeter**, Description of, 240.
- Photosensitization**
Bromine sensitized photodecomposition of ozone, 363.
Cadmium sensitized reactions of ethylene, 47.
Quenching of mercury resonance radiation by ethylene, 44.
- Plastein formation**, Problem of,
I. The formation of a plastein by papain, 255.
II. The chemical changes involved in plastein formation by papain and by pepsin, 272.
III. A note on the complexity of peptic plastein in urea solution, 305.
- Platinum** group in nickel ores and concentrates. Determination of the metals of the, 333.

Platinum, Massive Platinized glass as a laboratory substitute for, 318.

Polymers, The reaction of polystyrenes with bromine, 309.

Polystyrene(s)

Reaction with benzoyl hydrogen peroxide, 311.
bromine, 309.

Oxidation, 310.

Potassium carbonate

Activity coefficients in aqueous solution, 373.

pH of solutions of, at 25° C., 160, 164.

Pressures(s)

Effect on inhibition by nitric oxide of the thermal decomposition of *n*-butane, 2.

Equilibrium, of oxygen adsorbed on activated charcoal, 35.

Variation of density of gaseous chlorine with, 55.

Protopine from

Corydalis ochotensis, 78.

Corydalis claviculata, 98.

Corydalis nobilis, 291.

Corydalis pallida, 82.

Reaction velocity of

bromine sensitized photodecomposition of ozone, 363.

chemisorption of oxygen by charcoal, 35.

decomposition of hydrogen peroxide on glass and gold, 85, 87.

thermal decomposition of

benzylidene diacetate, *o*-chlorobenzylidene diacetate, benzylidene dibutyrate, 223.

n-butane (nitric oxide inhibited), 1.

ethane, 203.

ethane (nitric oxide inhibited), 351.

glyoxal tetra-acetate, 410.

Rhodium, Determination of, in nickel ores and concentrates, 341.

Riboflavin, Photoelectric colorimeter-fluorimeter in determination of, 240.

Ruthenium, Determination of, in nickel ores and concentrates, 338.

Scoulerine, Ethylation and degradation, 415.

Selenium

content of Saskatchewan wheat, 138.

Relation of occurrence of, to soil type, 149.

Silver, Determination of, in nickel ores and concentrates, 342.

Sinactine (Alkaloid F36), Oxidation of, 101.

Sodium carbonate

Activity coefficients in aqueous solution, 373.

pH of solutions of, at 25° C., 160, 164.

Sodium hydroxide, Heat of adsorption of, by mercerized and standard cottons, 170.

Sodium hypobromite, Action on

benzylphenylsuccinamide, 95.

hexylphenylsuccinamide, 94.

methylphenylsuccinamide, 92.

Soil type, Saskatchewan, Relation of occurrence of selenium to, 149.

Solid solutions of hydrogen peroxide and water, 66.

Solubility measurements in the region of the critical temperature, 293.

Specific volumes of hydrogen-peroxide-water mixtures, 191.

Stedman columns, Fractionation of Turner Valley crude oils using, 12, 388.

Stylopine from

Corydalis claviculata, 98.

Corydalis nobilis, 289.

Succinamide, Action of sodium hypobromite on,

α -Methyl- α' -phenyl-, 92.

α -*n*-Hexyl- α' -phenyl-, 94.

α -Benzyl- α' -phenyl-, 95.

Succinic acid

α -Benzyl- α' -phenyl-, 95.

α -*n*-Hexyl- α' -phenyl-, 94.

α -Methyl- α' -phenyl-, 91.

Succinic acids, Substituted, Derivatives of, IV. The action of alkaline sodium hypobromite on some α -alkyl- α' -aryl-succinamides, 90.

Succinimide

α -Methyl- α' -phenyl-, 92.

α -*n*-Hexyl- α' -phenyl-, 94.

α -Benzyl- α' -phenyl-, 95.

Sulphar ilamide, Enzyme inhibition by derivatives of phenothiazine and of, 345.

Sulphuric acid method in determination of metals of platinum group in nickel ores, 336.

Temperature

- Critical dispersion (critical region), 118.
- Effect on inhibition by nitric oxide of thermal decomposition of *n*-butane, 4.
- Variation of density of gaseous chlorine with, 55.
- Variation of viscosity of ethylene with, 135.
- viscosity-density relations of carbon dioxide in critical region, 326.
- See Critical temperature region.

d-Tetrahydro-palmatine, from

- Corydalis nobilis*, 289.
- Corydalis pallida*, 81.

dl-Tetrahydro-palmatine, from

- Corydalis nobilis*, 289.
- Corydalis pallida*, 81.

Thermal decomposition of

- benzylidene diacetate, benzylidene dibutyrate, and *o*-chlorobenzylidene diacetate, 223.
- butane, 1.
- ethane, 351, 203.
- glyoxal tetra-acetate, 410.

Thiamin, Photoelectric colorimeter-fluorimeter in determination of, 240.

Tocopherol content of oils, A proposed modification of Emmerie's method for determining, 405.

Turner Valley crude oil, Fractionation of, using Stedman columns, 12, 388.

Ultra-violet absorption spectra of samples of Turner Valley crude oil containing aromatics, 25.

Uracil, 5-Methyl-6-phenyl-dihydro-, 92, 93.

Urea solution, Complexity of peptic plastein in, 305.

Vanillin, Action of ozone on, in ethyl acetate, 33. in formic acid, 33.

Vaporization, Latent heat of, of hydrogen-peroxide-water mixtures, 189.

Vapour pressures of binary mixtures of hydrogen peroxide and water, 181.

Velocity distribution of gaseous molecules, 123.

Veratric aldehyde, Action of ozone on, in ethyl acetate, 34. in formic acid, 34.

Viscosity

- in the critical region. Ethylene, Measurement of, 128.
- of carbon dioxide in the critical region, 322.

Vitamin B₁, See Thiamin.

Vitamin B₂, See Riboflavin.

Water(s)

- Alberta, Determination of fluorine in, 151.
- Heat of wetting of mercerized cotton by, 171.
- Heavy, Catalytic decomposition of hydrogen peroxide in, 84.
- on glass, 84.
- on gold, 87.

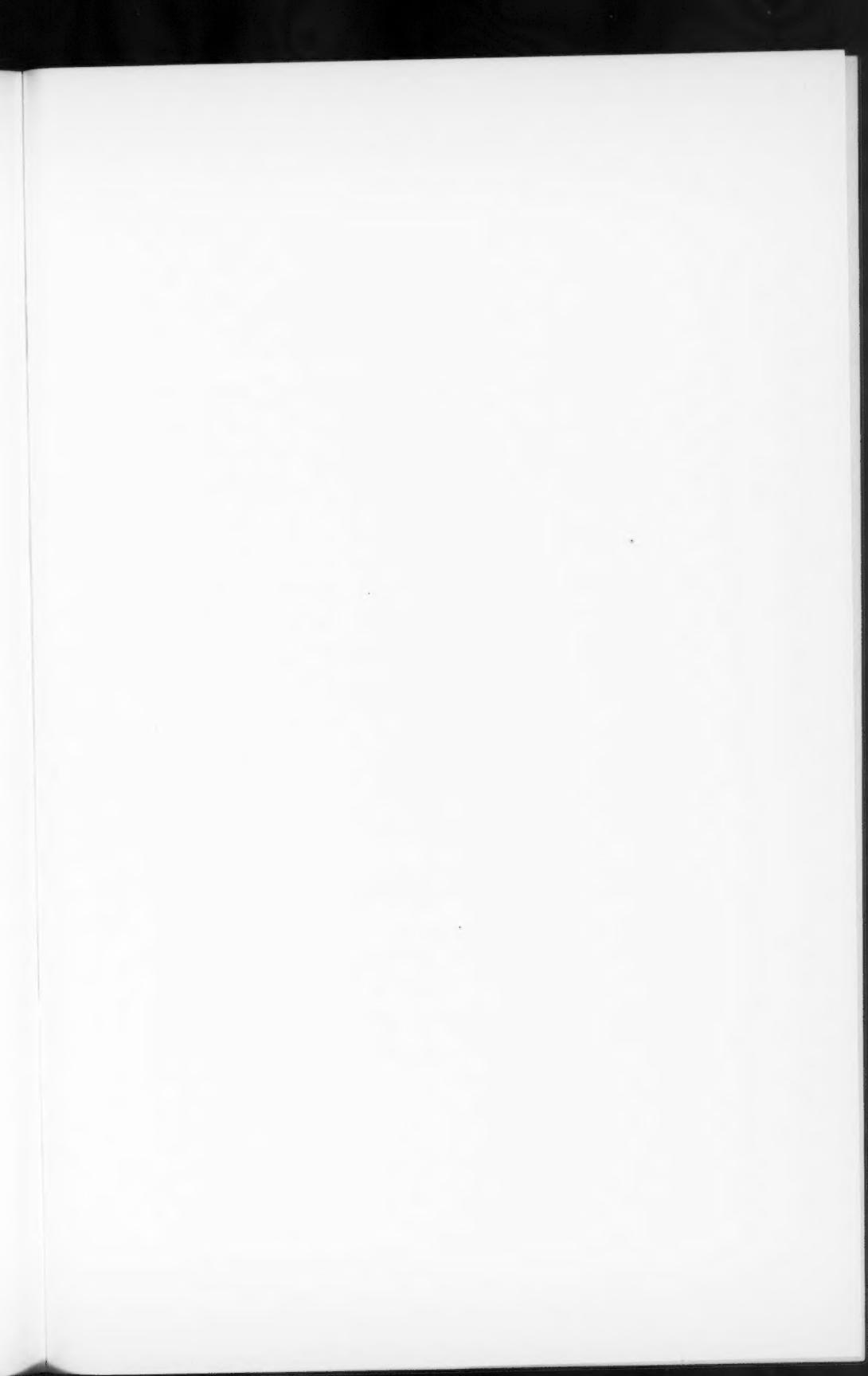
Water and hydrogen peroxide

- Solid solutions of, 66.
- Vapour pressures and boiling points of binary mixtures of, 181.

Wetting, Heat of, of mercerized celluloses by sodium hydroxide solutions, water, and methyl alcohol, 168.

Wheat, Saskatchewan, Selenium content of, 138.

Wheat flour films, Gelation phenomena in, 194.





CANADIAN JOURNAL OF RESEARCH

Notes on the Preparation of Copy

General:—Manuscripts should be typewritten, double spaced, and the original and one copy submitted. Style, arrangement, spelling, and abbreviations should conform to the usage of this Journal. Names of all simple compounds, rather than their formulae, should be used in the text. Greek letters or unusual signs should be written plainly or explained by marginal notes. Superscripts and subscripts must be legible and carefully placed. Manuscripts should be carefully checked before being submitted, to reduce the need for changes after the type has been set. All pages should be numbered.

Abstract:—An abstract of not more than about 200 words, indicating the scope of the work and the principal findings, is required.

Illustrations:—Drawings should be carefully made with India ink on white drawing paper, blue tracing linen, or co-ordinate paper ruled in blue only. Paper ruled in green, yellow, or red should not be used. The principal co-ordinate lines should be ruled in India ink and all lines should be of sufficient thickness to reproduce well. Lettering and numerals should be of such size that they will not be less than one millimetre in height when reproduced in a cut three inches wide. If means for neat lettering are not available, lettering should be indicated in pencil only. All experimental points should be carefully drawn with instruments.

Illustrations need not be more than two or three times the size of the desired reproduction, but the ratio of height to width should conform with that of the type page. Small photographs should be mounted on cardboard and those to be reproduced in groups should be so arranged and mounted. The author's name, title of paper, and figure number should be written on the back of each illustration. Captions should not be written on the illustrations, but typed on a separate page of the manuscript.

Tables:—Titles should be given for all tables, which should be numbered in Roman numerals. Column heads should be brief and textual matter in tables confined to a minimum.

References should be listed alphabetically by authors' names, numbered in that order, and placed at the end of the paper. The form of literature citation should be that used in this Journal and titles of papers should not be given. All citations should be checked with the original articles.

The *Canadian Journal of Research* conforms in general with the practice outlined in the *Canadian Government Editorial Style Manual*, published by the Department of Public Printing and Stationery, Ottawa.



